

AD 69268

# DIRECTIONAL RADIANCE (Luminance) OF THE SEA SURFACE

SIO REF. 69-20  
October 1969

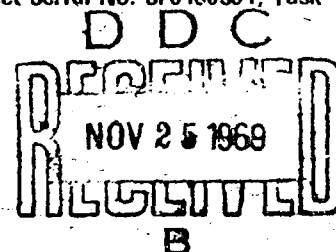
Jacqueline I. Gordon

DISTRIBUTION OF THIS DOCUMENT IS UNLIMITED



Reproduced by the  
CLEARINGHOUSE  
for Federal Scientific & Technical  
Information Springfield Va. 22151

Naval Ship Systems Command  
Washington, D. C. 20360  
Contract N00024-68-C-1100, Task I  
Project Serial No. SF0100301, Task 11632



VISIBILITY LABORATORY San Diego, California 92152

This document has been approved  
for public release and sale; its  
distribution is unlimited

56

UNIVERSITY OF CALIFORNIA, SAN DIEGO  
SCRIPPS INSTITUTION OF OCEANOGRAPHY  
VISIBILITY LABORATORY  
SAN DIEGO, CALIFORNIA 92152

**DIRECTIONAL RADIANCE (LUMINANCE) OF THE SEA SURFACE**

Jacqueline I. Gordon


DISTRIBUTION OF THIS DOCUMENT IS UNLIMITED

SIO Ref. 69-20


October 1969

Naval Ship Systems Command  
Department of the Navy  
Washington, D. C. 20360  
Project Serial No. SF0100301, Task 11632

Approved:

  
Seibert Q. Duntley, Director  
Visibility Laboratory

Approved for Distribution:

  
William A. Nierenberg, Director  
Scripps Institution of Oceanography

## Contents

PREFACE	i
1. INTRODUCTION	1
2. CALM WATER	2
2.1 Fresnel Reflectance and Transmittance	2
2.2 Index of Refraction of Sea Water	3
2.3 Sky and Sun Reflectance	5
2.4 Upwelling Radiance (Luminance)	6
2.4.1 Downwelling Irradiance (Illuminance) Beneath the Water Surface	6
2.4.2 Upwelling Radiance (Luminance) Beneath the Water Surface	7
2.4.3 Upwelling Radiance (Luminance) Above the Water Surface	12
2.5 Directional Radiance (Luminance) of Calm Water	13
3. WIND-RUFFLED SEA, AVERAGED	14
3.1 Wave Slope Statistics	14
3.2 Ergodic Cap	16
3.2.1 Rotation of Coordinate Systems	18
3.3 Occultation from Light Sources	20
3.4 Sun Glitter	21
3.5 Sky Reflectance	24
3.6 Upwelling Light	27
3.6.1 Time-averaged Transmittance and Cosine	28
3.6.2 Time-averaged Internal Reflectance of Diffuse Light	31
3.6.3 Time-averaged Transmittance	33
3.7 Directional Radiance (Luminance) of the Time-averaged Wind-ruffled Sea	34
4. RADIANCE (LUMINANCE) PATTERNS OF LARGE WAVES	34
4.1 Tipped Ergodic Cap	35
4.2 Sun Glitter	36
4.3 Sky Reflectance	37
4.4 Upwelling Radiance	40
4.5 Directional Radiance of Tilted Sea Surface	40
5. REFERENCES	40

## Appendices

A. Derivation of Equations for the Transformation of Rotation of Axes Expressed in Spherical Coordinates by J. W. Wasserboehr and J. I. Gordon	42
B. Occlusion by Keith B. MacAdam	46

## PREFACE

This report is an integration and extension of concepts developed under several earlier Visibility Laboratory contracts.

The first of these, N5ori-07831, N5ori-07864, and NObs-50378 were contracts between the United States Navy and the Massachusetts Institute of Technology when, prior to 1952, the Visibility Laboratory was a part of that institution (see reference 1, entitled "The Visibility of Submerged Objects"). Another, much later contract, NObs-84075 (Assignment 1), concerned the night aerial search for aviators downed at sea for the U. S. Navy Bureau of Naval Weapons. Three other contracts, NObs-84075 (Assignment 3), NObs-92058 (Task 1), and NObs-95251 (Task 1) concerned ocean surveillance from satellites for the Bureau of Ships. Still another, Nonr-2216 (Tasks 25 and 27), studied the appearance of water wave patterns for the Office of Naval Research. Finally contract NObs-84075 (Assignment 9) provided for the development and reporting of technical materials useful for visibility calculations.

The writing of this report was accomplished partially under Assignment 9 of Contract NObs-84075 and partially under Task 1 of NObs-95251. Final editing, reproduction and distribution was accomplished under Contract N00024-68-C-1100, Task 1 to which the subject matter of the report contributes directly as an integral part of the Laboratory's "investigation of the detectability and recognizability of military targets in the sea environment".

# **DIRECTIONAL RADIANCE (LUMINANCE) OF THE SEA SURFACE**

Jacqueline I. Gordon

## **1. INTRODUCTION**

Equations for the computation of directional sea radiance and/or luminance are presented. Three types of conditions for which the calculations may be made are each treated separately: first, the radiance or luminance of the calm sea; second, the unresolved radiance or luminance of the time- or space-averaged wind-ruffled sea; and third, the radiance or luminance of the sea surface in which the large wave pattern is resolved but the small capillary waves are unresolved.

This report is for the purpose of presenting the complete set of equations, with derivations, that are needed for the calculation of the directional sea radiance (luminance). The basis for the calculations in Sections 2 and 3 can be found in an earlier report by Duntley<sup>1</sup>. The extensions and modifications are in agreement with the theories and equations given by Preisendorfer<sup>2</sup>, but the treatment of the details of the sea radiance (luminance) computations given herein are in greater detail. Many of the equations in Section 4 also appear in the unclassified section of a final report for an ONR project<sup>3</sup>; no derivations were given there, however, so the present treatment, while parallel, contains modifications and is more complete.

Angular notation throughout is as follows: The zenith angle is designated by  $\theta$ . See Fig. 1. The azimuth is with reference to the azimuth of the sun and is noted by  $\phi$ . These angles are always given as parenthetic attachments to a radiance  $N$  or a luminance  $B$ , the angles thus denoting the direction of the path of sight of the photometer. The altitude is not included in the parenthesis since it is always sea level or zero in an inherent sea radiance or luminance computation

Radiance units used throughout are watts/ $\Omega$  sq. ft.; irradiance units are watts/sq. ft. Luminance units are in Ft-Lamberts and illuminance units are in lumens/sq. ft. The directional radiance of the sea surface would thus be  $N(\theta_p, \phi_p)$  and the luminance  $B(\theta_p, \phi_p)$ .

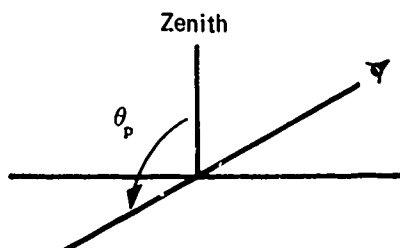


Fig. 1. Plane passed through path of sight and zenith.

The inherent radiance (luminance) of calm water will be discussed first, followed by the radiance (luminance) of the time- or space-averaged wind-ruffled sea surface. Next will be described the extension of these ideas to approximate the radiance (luminance) of the sea surface as it might appear in a photograph with, for example, a resolution of 1 ft.

A program for the CDC 3600 computer has been completed which carries out the computations herein described for calm water, the time-averaged wind-ruffled sea, and the tilted sea surface of intermediate resolution (in time- or space-averaging). This report contains the equations which are the basis of that program.

## 2. CALM WATER

The directional sea radiance (luminance) for calm water is the sum of the reflected radiance (luminance) of the sun or the sky and the upwelling radiance (luminance). The radiance upwelling from within the sea results from sunlight and skylight which has been transmitted downward through the air-water surface, scattered upward by the (optically infinite) deep water, and then transmitted through the water-air surface toward the sensor.

The reflectance and transmittance of the air-water surface will be reviewed first, followed by a discussion of the index of refraction of the ocean surface. Next, the equations for computing the sky or sun reflectance will be presented. Then the upwelling radiance (luminance) will be investigated.

Most of the equations in this section come directly from Reference 1. They are reproduced here not only for convenience but also to allow certain necessary modifications to be made.

### 2.1 Fresnel Reflectance and Transmittance

The Fresnel reflectance,  $r(\theta)$ , and transmittance,  $t(\theta)$ , are dependent on the index of refraction of the water,  $n'$ , the index of refraction of the air,  $n$ , and the zenith angle of the incident radiation,  $\theta$ .

The refracted angle,  $\Theta$ , see Fig. 2, beneath the water surface is defined by Snell's Law to be

$$\Theta = \sin^{-1} [(n/n') \sin \theta] \quad (2.1.1)$$

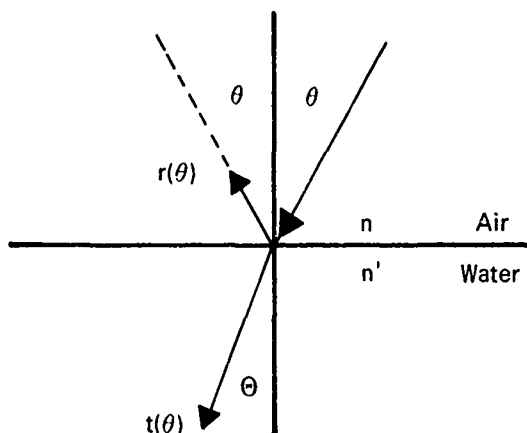


Fig. 2. Reflection, transmission, and refraction.

The Fresnel reflectance,  $r(\theta)$ , can be found as follows:

$$r(\theta) = [\tan^2 (\theta - \Theta)/2 \tan^2 (\theta + \Theta)] + [\sin^2 (\theta - \Theta)/2 \sin^2 (\theta + \Theta)] \quad (2.1.2)$$

The proportion of the radiation transmitted through the surface is,

$$t(\theta) = 1 - r(\theta) \quad (2.1.3)$$

The index of refraction of air,  $n = 1$ .

## 2.2 Index of Refraction of Sea Water

The index of refraction of the surface sea water depends upon the wavelength of the incident radiation; and upon the water temperature and salinity. The temperature range is  $-2^\circ$  to  $+30^\circ\text{C}$ . The normal salinity range is from 33 to 37 parts per mille.<sup>4</sup> The effect of salinity and temperature in these ranges is an order of magnitude less than the effect of wavelength of the incident light. Therefore it is reasonable to use the index of refraction for water with a salinity of 35 parts per mille which is the average for the open ocean. Also it is reasonable to use a water temperature of  $20^\circ\text{C}$  (only other data by wavelength available was at  $0^\circ$  and  $40^\circ\text{C}$ ).

The index of refraction at various wavelengths is given in Table 1 for distilled water at 20°C.<sup>5</sup> The index of refraction for sea water with a salinity of 35 parts per mille at 20°C is given in the same table for the sodium-D wavelength, 0.589  $\mu\text{m}$ .<sup>6</sup> The values for the other wavelengths for sea water were estimated by multiplying the distilled water values by factors. A factor was obtained for each wavelength from the distilled water data at 20°C from the ratio of the index for that wavelength to the index for sodium. The factor for 0.546  $\mu\text{m}$ , mercury, was given in Ref. 6

The indices in Table 1 are depicted graphically in Fig. 3. Indices of refraction for intermediate wavelengths can be found by interpolating between the values given. The suggested index of refraction for photopic calculations for seawater is 1.341.

Table 1. Indices of refraction of water.\*

	Temperature °C	Salinity ‰	Wavelength ( $\mu\text{m}$ )					
			0.397	0.434	0.486	0.546	0.589	0.656
Distilled water	20	0	1.3435	1.3404	1.3372	1.3345	1.3330	1.3312
Sea water	20	35	(1.3500)	(1.3468)	(1.3436)	(1.3409)	1.3394	(1.3376)

\* Values in parentheses are estimated.

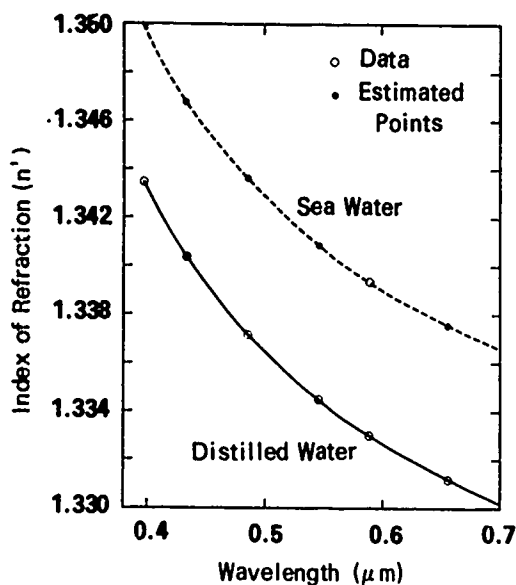


Fig. 3. Index of refraction of sea water and distilled water.



### 2.3 Sky and Sun Reflectance

The calm water reflects the radiance from the sky or sun which is at the angular position  $\theta_B, \phi_B$  into the path of sight at  $\theta_p, \phi_p$ .

$$N_{\text{sky or sun}}(\theta_p, \phi_p) = N(\theta_B, \phi_B) r(\theta_B) \quad (2.3.1)$$

The reflectance  $r(\theta_B)$  is the Fresnel reflectance at angle  $\theta_B$ .

The sky or sun position  $\theta_B, \phi_B$  is in the same azimuth as path of sight  $\phi_p$  but at the zenith angle of the observer position  $\theta_o$ . The path of sight zenith angle,  $\theta_p$ , and azimuth,  $\phi_p$ , are in the opposite direction from the sensor or observer position zenith angle,  $\theta_o$ , and azimuth,  $\phi_o$ . Thus,

$$\phi_B = \phi_p = \phi_o + 180^\circ \quad (2.3.2)$$

$$\theta_B = \theta_o = 180^\circ - \theta_p \quad (2.3.3)$$

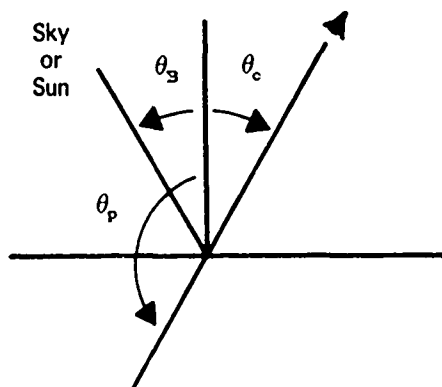


Fig. 4. Plane passed through the path of sight and the zenith.

Equation (2.3.1) can be rewritten in terms of  $\theta_o$  and  $\phi_p$ .

$$N_{\text{sky or sun}}(\theta_p, \phi_p) = N(\theta_o, \phi_p) r(\theta_o) \quad (2.3.4)$$

The sun will be reflected when  $\theta_o = \theta_s$  and  $\phi_p = 0$ ; thus

$$N_{sun}(180^\circ - \theta_s, 0) = \bar{N}_s(\theta_s, 0) r(\theta_s) \quad (2.3.5)$$

where  $\bar{N}_s(\theta_s, 0)$  is the apparent sun radiance averaged over the solar disk.

The photopic equations are directly analogous as follows:

$$B_{sky \text{ or } sun}(\theta_p, \phi_p) = B(\theta_o, \phi_p) r(\theta_o) \quad (2.3.6)$$

and

$$B_{sun}(180^\circ - \theta_s, 0) = \bar{B}_s(\theta_s, 0) r(\theta_s) \quad (2.3.7)$$

## 2.4 Upwelling Radiance (Luminance)

The upwelling radiance (luminance) is light from the sun and sky which has gone through three processes. First, the light is transmitted through the air-water surface. The downwelling irradiance (illuminance) is the light measured just beneath the ocean surface by an irradiator (illuminometer). Second, some of the downwelling irradiance is reflected by the (optically infinite) deep water, and interreflected between the water-air surface and the deep water. The upwelling radiance (luminance) just beneath the water surface in the appropriate direction for the sensor's (observer's) path of sight, results from these reflections. Third, the upwelling radiance (luminance) is transmitted through the water-air surface into the path of sight of the sensor (observer). This is the upwelling radiance (luminance) as measured just above the water surface.

### 2.4.1 DOWNWELLING IRRADIANCE (ILLUMINANCE) BENEATH THE WATER SURFACE.

The sky radiance,  $N(\theta_B, \phi_B)$ , from a solid angle,  $d\Omega$ , and projected area,  $ds \cos\theta_B$ , enters the water at an angle  $\theta_B$ . The proportion entering is  $t(\theta_B)$ .

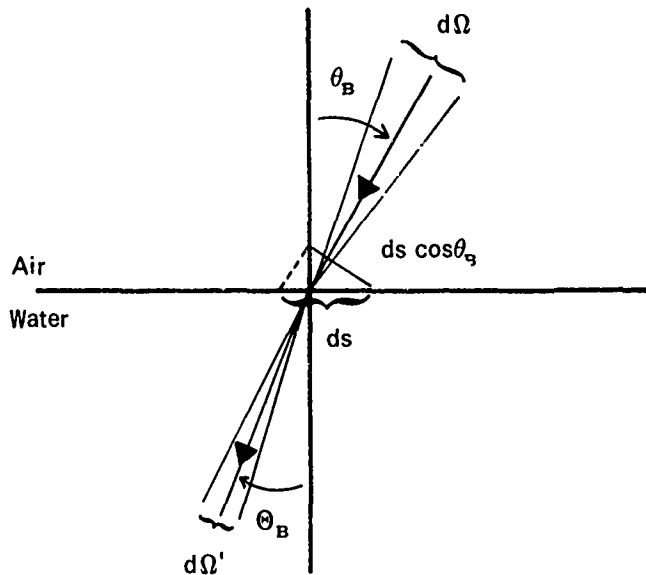


Fig. 5. Transmittance geometry.

The radiance just beneath the surface,  $N(\Theta_B, \phi_B)$  is related to the radiance above the surface by the ratio of the respective solid angles and projected areas, and by the transmittance  $t(\theta_B)$ , see Fig. 5.

$$N(\Theta_B, \phi_B) = N(\theta_B, \phi_B) t(\theta_B) \frac{ds \cos \theta_B d\Omega}{ds \cos \Theta_B d\Omega'} \quad (2.4.1)$$

A flat plate collector will receive this sky radiance,  $N(\Theta_B, \phi_B)$ , at the refracted angle,  $\Theta_B$ . The collector will weight the amount received by  $\cos \Theta_B d\Omega'$ . The downwelling irradiance beneath the water surface,  $H_D(0,0)^*$  is thus,

$$H_D(0,0) = \int_{2\pi} N(\Theta_B, \phi_B) \cos \Theta_B d\Omega' \quad (2.4.2)$$

Substituting from Eq. (2.4.1) for  $N(\Theta_B, \phi_B)$ ,

$$H_D(0,0) = \int_{2\pi} N(\theta_B, \phi_B) t(\theta_B) \cos \theta_B d\Omega \quad (2.4.3)$$

The downwelling irradiance can also be expressed as a double summation, with  $\Delta \Omega_B = \sin \theta_B \Delta \theta_B \Delta \phi_B$ . Thus, Eq. 2.4.3 becomes,

$$H_D(0,0) = \sum_{i=1}^n \left[ \sum_{j=1}^m N(\theta_{Bi}, \phi_{Bj}) \Delta \phi_{Bj} \right] t(\theta_{Bi}) \cos \theta_{Bi} \sin \theta_{Bi} \Delta \theta_{Bi} \quad (2.4.4)$$

The sun contribution can be treated as a separate term, in an analogous fashion. Therefore, the total downwelling irradiance from sun and sky would be,

$$H_D(0,0) = \int_{2\pi} N(\theta_B, \phi_B) t(\theta_B) \cos \theta_B d\Omega_B + \bar{N}_s(\theta_s, 0) t(\theta_s) \cos \theta_s d\Omega_s \quad (2.4.5)$$

where  $d\Omega_s$  is the solid angle of the solar disk;  $d\Omega_s = 6.8193 \times 10^{-5}$  steradians at mean solar distance. The maximum variability in  $d\Omega_s$ , at the perihelion and aphelion, is  $\pm 3.4$  percent.

The equation for the downwelling illuminance beneath the water surface has an analogous derivation; but it contains a  $\pi$  term since the luminances used are in ft-L.

$$E_D(0,0) = \frac{1}{\pi} \left[ \int_{2\pi} B(\theta_B, \phi_B) t(\theta_B) \cos \theta_B d\Omega_B + \bar{B}_s(\theta_s, 0) t(\theta_s) \cos \theta_s d\Omega_s \right] \quad (2.4.6)$$

#### 2.4.2 UPWELLING RADIANCE (LUMINANCE) BENEATH THE WATER SURFACE

The reflectance of the (optically infinite) deep water is a function of wavelength. It is measured just beneath the water surface by two flat plate collectors: one measuring the upwelling spectral irradiance  $H_U(180,0)$  and one measuring the downwelling spectral irradiance  $H_D(0,0)$ .

\* The parenthetic expression (0,0) denotes the zenith angle and azimuth of the normal vector from the surface of the irradiator.

$$R_{\infty}(\lambda) = \frac{H_u(180,0)}{H_D(0,0)} \quad (2.4.7)$$

The photopic deep water reflectance is defined by the ratio of the upwelling illuminance to the downwelling illuminance.

$$R_{\infty}(\bar{y}) = \frac{E_u(180,0)}{E_D(0,0)} \quad (2.4.8)$$

The deep water reflectance is a function of the water clarity as well as wavelength. The standard photopic value for deep water reflectance is 0.02 but values ranging from 0.01 to 0.15 have been reported.<sup>7</sup>

The reflectance of deep water as a function of wavelength is given in Table 2, and Fig. 6. The curve represents measurements made with a spectrogeograph in a glass-bottomed boat in the Gulf Stream off Dania, Florida.<sup>8,9,10</sup> Values below 0.420  $\mu\text{m}$  and above 0.570  $\mu\text{m}$  are extrapolated. Note that  $R_{\infty}(0.550) \neq 0.02$ . The photopic deep water reflectance of 0.02 can be computed from the following equation; where the incoming radiation  $H_{\lambda}$  is the solar spectral radiation from Johnson.<sup>11</sup>

$$R_{\infty}(\bar{y}) = \frac{\int_0^{\infty} R_{\infty}(\lambda) H_{\lambda} \bar{y}_{\lambda} d\lambda}{\int_0^{\infty} H_{\lambda} \bar{y}_{\lambda} d\lambda} \quad (2.4.9)$$

The reflectance of (optically infinite) deep water for a radiometric sensor having a broad band spectral sensitivity of  $S_{\lambda}$  would be computed in a similar manner.

Table 2. Reflectance of (optically infinite) deep water.\*

Wavelength ( $\mu\text{m}$ )	$R_{\infty}(\lambda)$	Wavelength ( $\mu\text{m}$ )	$R_{\infty}(\lambda)$	Wavelength ( $\mu\text{m}$ )	$R_{\infty}(\lambda)$
0.40	(0.075)	0.50	0.053	0.60	(0.0035)
0.41	(0.079)	0.51	0.040	0.61	(0.0029)
0.42	0.082	0.52	0.034	0.62	(0.0025)
0.43	0.086	0.53	0.028	0.63	(0.0022)
0.44	0.090	0.54	0.022	0.64	(0.0020)
0.45	0.093	0.55	0.016	0.65	(0.0018)
0.46	0.096	0.56	0.012	0.66	(0.0017)
0.47	0.095	0.57	0.0079	0.67	(0.0016)
0.48	0.089	0.58	(0.0057)	0.68	(0.0015)
0.49	0.074	0.59	(0.0044)	0.69	(0.0014)
				0.70	(0.0014)

\* Values in parenthesis are extrapolated.

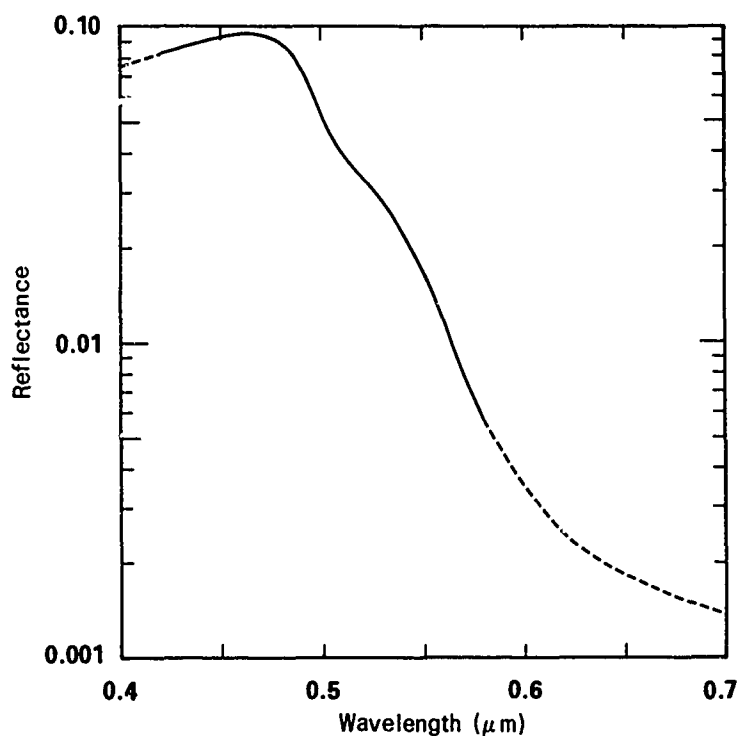


Fig. 6. Reflectance of (optically infinite) deep water.

Assuming the reflectance of the (optically infinite) deep water to be diffuse\*, the radiance reflected in all upward directions,  $N_{\uparrow}$ , is

$$N_{\uparrow} = H_D(0,0) \frac{R_{\infty}}{\pi} \quad (2.4.10)$$

This radiance strikes the water-air surface and reflects at angle  $\Theta$ . Some of the radiance is transmitted through the surface, the proportion reflected is  $r(\Theta)$  [ $r(\Theta) = r(\theta)$  where the relationship between  $\theta$  and  $\Theta$  is defined by Snell's Law, see Fig. 7].

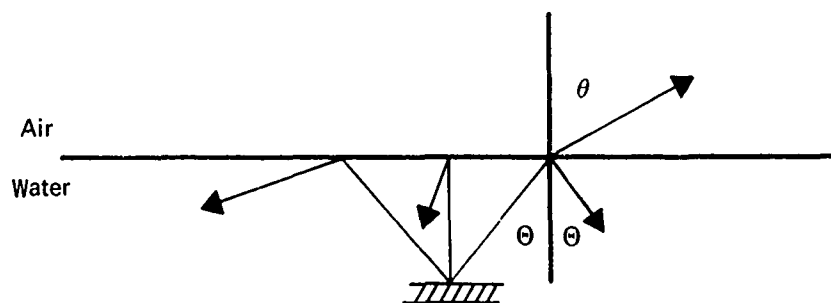


Fig. 7. Upwelling radiance reflected at  $\Theta$  by amount  $r(\theta)$ .

\* Strictly speaking, the reflectance is not diffuse but not enough data on the directional reflectance is available to allow the reflectance to be handled as other than diffuse. See Ref. 10, Fig. 26

The downward directed radiance  $N(\Theta, \phi)$  would thus be

$$N(\Theta, \phi) = N_{\uparrow} r(\Theta) \quad (2.4.11)$$

The downwelling irradiance from the first water-air surface reflectance would be:

$$H_{D1}(0, 0) = \int_{2\pi} N(\Theta, \phi) \cos\Theta \, d\Omega' \quad (2.4.12)$$

Substituting from Eq. 2.4.10 and 2.4.11.

$$H_{D1}(0, 0) = \frac{H_D(0, 0) R_{\infty}}{\pi} \int_{2\pi} r(\Theta) \cos\Theta \, d\Omega' \quad (2.4.13)$$

The reflectance of the diffuse upwelling light by the water-air interface is the emergent reflectance or internal reflectance,  $r_s$ . Thus,

$$r_s = \frac{1}{\pi} \int_{2\pi} r(\Theta) \cos\Theta \, d\Omega' \quad (2.4.14)$$

Using a discrete summation method, with  $\Delta\theta = 5^\circ$  and  $\Delta\phi = 10^\circ$ ,  $r_s$  has been evaluated to be 0.485 for the photopic index of refraction of sea water ( $n' = 1.341$ ). This is within 1 percent of the value reported by Judd<sup>12</sup> ( $n' = 1.34$ ,  $r_s = 0.480$ ) who used a smaller summative interval ( $\Delta\theta = 2.3^\circ$  except for the interval near the critical angle). The emergent reflectance for fresh water and salt water for all wavelengths in the visible spectrum varies less than 1 percent from the photopic value for sea water.

The downwelling irradiance from the first water-air surface reflectance can now be written thus:

$$H_{D1}(0, 0) = H_D(0, 0) R_{\infty} r_s \quad (2.4.15)$$

The downwelling irradiance from the second water-air surface reflectance would be

$$H_{D2}(0, 0) = H_{D1}(0, 0) R_{\infty} r_s = H_D(0, 0) (R_{\infty} r_s)^2 \quad (2.4.16)$$

Similarly the third and succeeding surface reflectances would be

$$H_{D3}(0, 0) = H_D(0, 0) (R_{\infty} r_s)^3 \quad (2.4.17)$$

$$H_{Dn}(0, 0) = H_D(0, 0) (R_{\infty} r_s)^n \quad (2.4.18)$$

The radiance which is in the direction which will be refracted toward the sensor's path of sight  $\theta_p$  is:

$$N(\Theta_p, \phi_p) = H_D(0, 0) \frac{R_{\infty}}{\pi} + H_{D1}(0, 0) \frac{R_{\infty}}{\pi} + H_{D2}(0, 0) \frac{R_{\infty}}{\pi} + \dots \quad (2.4.19)$$

or

$$N(\Theta_p, \phi_p) = H_D(0,0) \frac{R_\infty}{\pi} + H_D(0,0) \frac{R_\infty}{\pi} (R_\infty r_s) + H_D(0,0) \frac{R_\infty}{\pi} (R_\infty r_s)^2 + \dots \quad (2.4.20)$$

Let  $R_\infty r_s = x$ , then

$$N(\Theta_p, \phi_p) = H_D(0,0) \frac{R_\infty}{\pi} (1 + x + x^2 + x^3 + \dots) \quad (2.4.21)$$

The sum of the series in the parenthesis is  $1/(1-x)$ , therefore

$$N(\Theta_p, \phi_p) = H_D(0,0) \frac{R_\infty}{\pi (1 - r_s R_\infty)} \quad (2.4.22)$$

Substituting Eq. (2.4.5) in the above equation,

$$N(\Theta_p, \phi_p) = \left[ \frac{\int_{2\pi} N(\theta_B, \phi_B) t(\theta_B) \cos \theta_B d\Omega_B + \bar{N}_s(\theta_s, 0) t(\theta_s) \cos \theta_s d\Omega_s}{\pi (1 - r_s R_\infty)} \right] R_\infty \quad (2.4.23)$$

The equivalent derivation of the upwelling luminance beneath the water surface is as follows

$$B \uparrow = E_D(0,0) R_\infty \quad (2.4.24)$$

Note the  $\pi$  term is missing since the luminances are in ft-L.

$$B(\Theta, \phi) = B \uparrow r(\theta) \quad (2.4.25)$$

$$E_{D1}(0,0) = \frac{1}{\pi} \int_{2\pi} B(\Theta, \phi) \cos \Theta d\Omega' = E_D(0,0) R_\infty r_s \quad (2.4.26)$$

and

$$E_{D2}(0,0) = E_D(0,0) (R_\infty r_s)^2 \quad (2.4.27)$$

thus

$$B(\Theta_p, \phi_p) = E_D(0,0) R_\infty + E_{D1}(0,0) R_\infty + E_{D2}(0,0) R_\infty + \dots \quad (2.4.28)$$

and

$$B(\Theta_p, \phi_p) = E_D(0,0) R_\infty + E_D(0,0) R_\infty (R_\infty r_s) + E_D(0,0) R_\infty (R_\infty r_s)^2 + \dots \quad (2.4.29)$$

and

$$B(\Theta_p, \phi_p) = E_D(0,0) \frac{R_\infty}{(1 - r_s R_\infty)} \quad (2.4.30)$$

Note the  $\pi$  term is missing in Eq. 2.4.30, but when Eq. 2.4.6 is substituted, Eq. 2.4.23 and 2.4.31 become equivalent with no  $\pi$  term differences.

$$B(\Theta_p, \phi_p) = \left[ \frac{\int_{2\pi} B(\theta_B, \phi_B) t(\theta_B) \cos \theta_B d\Omega_B + \bar{B}_s(\theta_s, 0) t(\theta_s) \cos \theta_s d\Omega_s}{\pi(1 - r_s R_\infty)} \right] R_\infty \quad (2.4.31)$$

#### 2.4.3 UPWELLING RADIANCE (LUMINANCE) ABOVE THE WATER SURFACE

The upwelling radiance just beneath the water surface,  $N(\Theta_p, \phi_p)$ , is transmitted through the surface, and refracted by that surface so that the same energy is spread over a larger solid angle. The projected area of the radiance is smaller, being a function of  $\cos \theta_o$  in the air, and of  $\cos \Theta_o$  in the water. The total effect is to reduce the radiance by the Fresnel transmittance  $t(\theta_o)$  and by the ratio of the respective solid angles and projected areas, see Fig. 8.

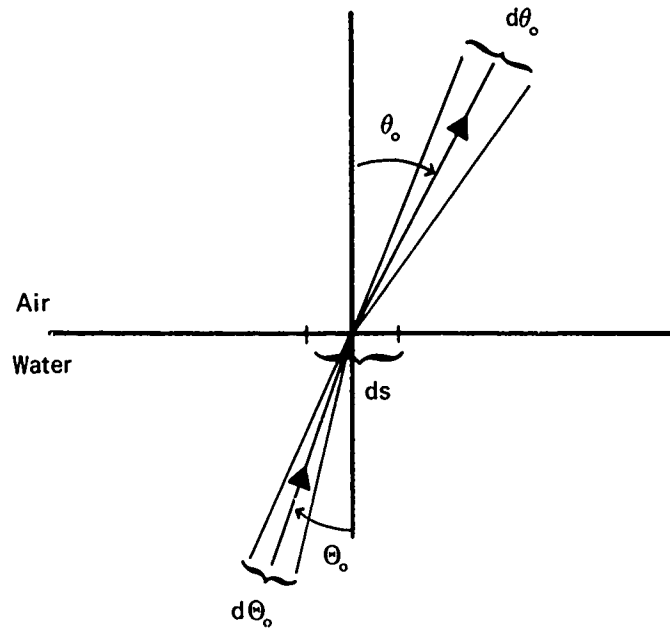


Fig. 8. Upwelling radiance at interface.



$$N_u(\theta_p, \phi_p) = N(\Theta_p, \phi_p) t(\theta_o) \frac{ds \cos \Theta_o d\Omega'}{ds \cos \theta_o d\Omega} \quad (2.4.32)$$

The solid angle of the radiance  $d\Omega$  may be written in the form  $\sin \theta_o d\theta_o d\phi$ . The azimuth  $d\phi$  does not change above and below the surface since  $\phi$  is defined by the plane through the light ray and the normal to the surface. Thus:

$$N_u(\theta_p, \phi_p) = N(\Theta_p, \phi_p) t(\theta_o) \frac{\cos \Theta_o \sin \Theta_o d\Theta_o}{\cos \theta_o \sin \theta_o d\theta_o} \quad (2.4.33)$$

To obtain  $d\Theta_o$ , Snell's law Eq. 2.1.1 is differentiated

$$\Theta_o = \sin^{-1} \left[ \frac{n}{n'} \sin \theta_o \right] \quad (2.1.1)$$

$$d\Theta_o = \frac{1}{\sqrt{1 - \left(\frac{n}{n'}\right)^2 \sin^2 \theta_o}} \frac{n}{n'} \cos \theta_o d\theta_o \quad (2.4.34)$$

by proper substitution,

$$d\Theta_o = \frac{n}{n'} \frac{\cos \theta_o}{\cos \Theta_o} d\theta_o \quad (2.4.35)$$

then since  $\sin \Theta_o / \sin \theta_o = n/n'$ , Eq. 2.4.33 becomes

$$N_u(\theta_p, \phi_p) = N(\Theta_p, \phi_p) t(\theta_o) \left( \frac{n}{n'} \right)^2 \quad (2.4.36)$$

The change in radiance at an interface due to the square of the ratio of the refractive indices was first noted by Gershun.<sup>13</sup>

The photometric expression for the upwelling luminance is directly comparable to Eq. 2.4.36.

## 2.5 Directional Radiance (Luminance) of Calm Water

The directional radiance of calm water  $N(\theta_p, \phi_p)$  is the sum of the reflected sky and/or sunlight and the upwelling radiance.

$$N(\theta_p, \phi_p) = N_{sky \text{ or sun}}(\theta_p, \phi_p) + N_u(\theta_p, \phi_p) \quad (2.5.1)$$

Similarly, for the photopic case

$$B(\theta_p, \phi_p) = B_{sky \text{ or sun}}(\theta_p, \phi_p) + B_u(\theta_p, \phi_p) \quad (2.5.2)$$

### 3. WIND-RUFFLED SEA, AVERAGED

The wind-ruffled sea has a myriad of tiny wave facets which reflect and transmit the sun and sky light. The time- or space-averaged radiance (luminance) of the surface of the wind-rumpled sea is dependent upon the statistics of the tiny capillary wave slopes. The statistical distribution of these wave facets will be examined in the first section. The representation of the slope characteristics of the wind blown sea by means of an ergodic cap will be described in the second section. Third, the occlusion from the sky or sun of a given point on the surface of the sea by other waves is analyzed. Then come sections on the equations for sun glitter, sky reflectance, upwelling light, and their sum total, the time- or space-averaged directional radiance (luminance) of the wind-disturbed ocean surface.

#### 3.1 Wave Slope Statistics

The distribution of the water wave slopes is a function of local wind speed. The relationship of the slopes to the wind speed has been measured by Duntley<sup>14</sup> mostly at a fresh water lake and by Cox and Munk<sup>15</sup> in the open ocean. In both cases the distribution was elliptical with the up-wind direction containing larger slopes than the cross-wind direction. The relationship of the standard deviation of the wave slopes to the wind speed is given below for up-wind and cross-wind for the open ocean. The wind speed,  $v$ , is in knots and is for a 41 ft. height, the anemometer height normally used by ships at sea.

$$\sigma_u^2 = 0.00162 \left( \frac{\text{hr.}}{\text{n.mi.}} \right) v \quad (3.1.1)$$

$$\sigma_c^2 = 0.000990 \left( \frac{\text{hr.}}{\text{n.mi.}} \right) v \quad (3.1.2)$$

The standard deviation for any azimuth from the wind direction  $\Phi$  other than up-wind,  $\Phi = 0^\circ$ , or cross-wind,  $\Phi = 90^\circ$ , can be found by,

$$\sigma_\Phi^2 = \frac{\sigma_u^2 \sigma_c^2}{\sigma_u^2 \sin^2 \Phi + \sigma_c^2 \cos^2 \Phi} \quad (3.1.3)$$

In order to simplify the calculation of the sea radiance (luminance) the wave slope distribution will be approximated by a circular rather than an elliptical probability function. This means that the slope distribution in the up-wind and cross-wind directions will be assumed to be equivalent. In doing so, to minimize the error, the standard deviation for a  $45^\circ$  angle from the wind will be used since this lies between the measured values for up-wind and cross-wind.

$$\sigma_{45^\circ}^2 = \frac{2 \sigma_u^2 \sigma_c^2}{\sigma_u^2 + \sigma_c^2} = 0.00123 \left( \frac{\text{hr.}}{\text{n.mi.}} \right) v \quad (3.1.4)$$

Also,

$$\sigma = 0.0351 \sqrt{v} \quad (3.1.5)$$

This means that the wave slope distribution will be represented three dimensionally as illustrated in Fig. 9.

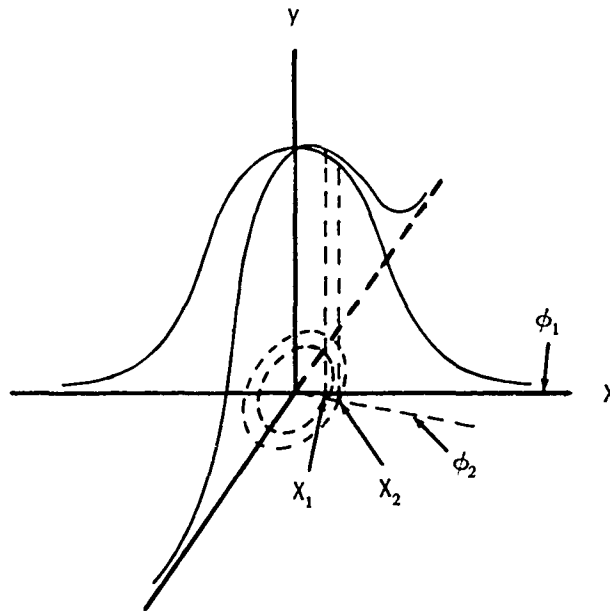


Fig. 9. Three-dimensional probability function.

Where the height,  $y$  is

$$y = \frac{1}{2\pi} \exp \left( -\frac{X^2}{2} \right) \quad (3.1.6)$$

and the radius  $X$  is

$$X = \frac{\tan \theta}{\sigma} \quad (3.1.7)$$

$\tan \theta$  is the wave slope. The volume  $V$  of the solid in Fig. 9 is the probability of the wave slopes. Thus, the total volume or total probability  $V = 1$ . From Fig. 9.

$$\Delta V = y\pi(X_2^2 - X_1^2) = \pi y(X_2 - X_1)(X_2 + X_1) \quad (3.1.8)$$

and

$$\Delta V = 2\pi y X \Delta X \quad (3.1.9)$$

therefore

$$V = \int_0^\infty X \exp \left( -\frac{X^2}{2} \right) dx = 1 \quad (3.1.10)$$

The probability  $V(\Delta\theta)$  that the wave slopes lie between  $\tan\theta_1$  and  $\tan\theta_2$  regardless of azimuth of orientation would be

$$V(\Delta\theta) = \int_{x_1}^{x_2} x \exp\left(-\frac{x^2}{2}\right) dx \quad (3.1.11)$$

$$= -\exp\left(-\frac{x_2^2}{2}\right) + \exp\left(-\frac{x_1^2}{2}\right) \quad (3.1.12)$$

Since  $x = \frac{\tan\theta}{\sigma}$

$$V(\Delta\theta) = -\exp\left(-\frac{\tan^2\theta_2}{2\sigma^2}\right) + \exp\left(-\frac{\tan^2\theta_1}{2\sigma^2}\right) \quad (3.1.13)$$

The probability,  $V(\Delta\theta, \Delta\phi)$ , that the wave slopes lie between  $\tan\theta_1$  and  $\tan\theta_2$ , and that the normal from the facets lies between  $\Phi_1$  and  $\Phi_2$  would be,

$$V(\Delta\theta, \Delta\phi) = \frac{(\phi_2 - \phi_1)}{2\pi} \left[ -\exp\left(-\frac{\tan^2\theta_2}{2\sigma^2}\right) + \exp\left(-\frac{\tan^2\theta_1}{2\sigma^2}\right) \right] \quad (3.1.14)$$

where  $\Delta\phi$  is in radians.

### 3.2 Ergodic Cap

The slope distribution of the wave facets for a given wind speed can be represented by a three-dimensional ergodic cap. The surface of the cap is shaped so that it has the correct distribution of slopes for that wind speed. The ergodic cap is circular since the probability function has been assumed to be circular.\* The horizontal projected area  $A_H$  of the ergodic cap is equated to the probability or volume under the three-dimensional probability function illustrated in Fig. 9. The total horizontal projected area thus equals 1.

\*The derivation for a non-circular ergodic cap has been made by Preisendorfer in Ref. 2. The cap becomes elliptical instead of circular but the general form of the equations is similar.

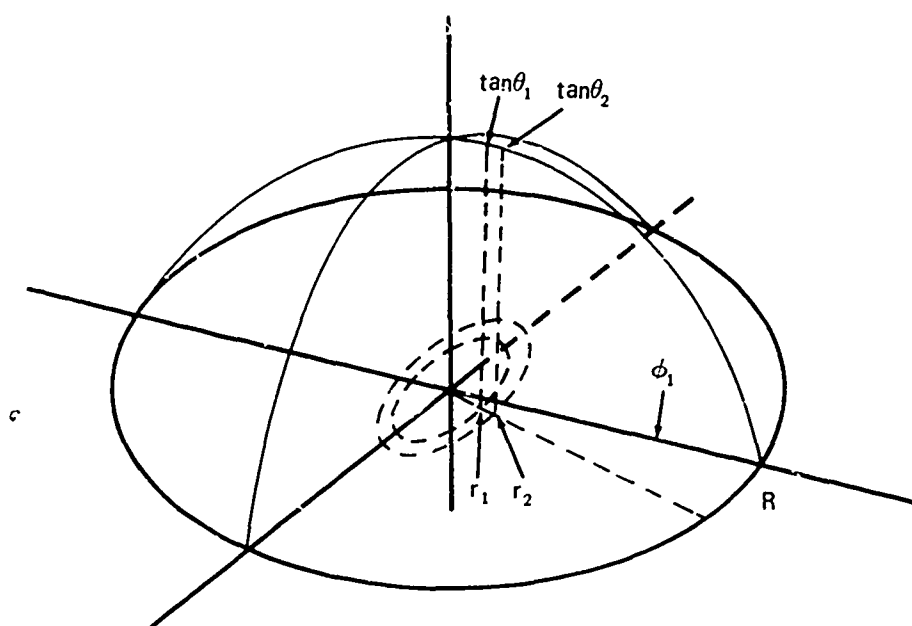


Fig. 10. Ergodic cap.

$$A_H = \pi R^2 = 1 \quad (3.2.1)$$

The portion of the ergodic cap which would have slopes between  $\tan \theta_1$  and  $\tan \theta_2$  in all azimuths would be between  $r_1$  and  $r_2$ , see Fig. 10, where,

$$A_H(\Delta \theta) = V(\Delta \theta) \quad (3.2.2)$$

$$\pi(r_2^2 - r_1^2) = -\exp\left(-\frac{\tan^2 \theta_2}{2\sigma^2}\right) + \exp\left(-\frac{\tan^2 \theta_1}{2\sigma^2}\right) \quad (3.2.3)$$

Also, the portion of the ergodic cap with slopes between  $\tan \theta_1$  and  $\tan \theta_2$  and with normals from the surface lying between  $\phi_1$  and  $\phi_2$  would be,

$$A_H(\Delta \theta, \Delta \phi) = V(\Delta \theta, \Delta \phi) \quad (3.2.4)$$

$$\frac{\Delta \phi}{2} (r_2^2 - r_1^2) = \frac{\Delta \phi}{2\pi} \left[ -\exp\left(-\frac{\tan^2 \theta_2}{2\sigma^2}\right) + \exp\left(-\frac{\tan^2 \theta_1}{2\sigma^2}\right) \right] \quad (3.2.5)$$

The true area of the surface of the cap with normals from the surface lying between  $\theta_1$  and  $\theta_2$ , and  $\phi_1$  and  $\phi_2$ , is

$$A_T(\Delta \theta, \Delta \phi) = \frac{A_H(\Delta \theta, \Delta \phi)}{\cos \theta_N} \quad (3.2.6)$$

where  $\theta_N$  is  $(\theta_1 + \theta_2)/2$  or the average slope of the elemental surface area.

The area as seen by an observer or sensor along an inclined path of sight at  $\theta_p, \phi_p$ , is equal to the true area projected onto the plane perpendicular to the path of sight. This projected area is equal to the true area times the cosine of the angle between the normal from the surface at  $\theta_N, \phi_N$  [where  $\phi_N = (\phi_1 + \phi_2)/2$ ] and the observer's position, at  $\theta_o, \phi_o$ . This angle is the Fresnel reflectance angle,  $\theta_R$ .

$$A_p(\Delta\theta, \Delta\phi) = A_T(\Delta\theta, \Delta\phi) \cos\theta_R \quad (3.2.7)$$

When  $\theta_r \geq 90^\circ$ ,  $A_p(\Delta\theta, \Delta\phi) = 0$ .

The elemental horizontal area of the ergodic cap,  $A_H(\Delta\theta, \Delta\phi)$ , is equivalent to the probability of occurrence of the wave slopes between  $\Delta\theta$  and  $\Delta\phi$ . The elemental projected area of the ergodic cap divided by the total projected area of the ergodic cap,  $A_p(\Delta\theta, \Delta\phi)/A_p$ , is the probability of occurrence of the radiance (luminance) reflected and transmitted by the elemental surface area in the direction of the path of sight of the observer.

The ergodic cap will be used to develop the geometry of the reflectance and transmittance of the sun, sky, and upwelling light. The probability function will be used to give the probability of occurrence of the wave slopes. The ergodic cap will be used as a continuously curved surface for development of the equations for reflectance and transmittance of the sun by the water surface. The reflectance and transmittance of the sky light, however, will be handled by a simplified ergodic cap, having, instead of a continuously curved surface, a series of flat surfaces, each having a normal from the surface at angle  $\theta_N, \phi_N$ .

### 3.2.1 ROTATION OF COORDINATE SYSTEMS

Computation of the reflectance (transmittance) angle for each ergodic cap element, and the position  $\theta_B, \phi_B$  of the sky radiance (luminance) reflected (or transmitted) is facilitated by using unit vector notation, the normal from the surface being  $\tilde{N}$ , the sky position being  $\tilde{B}$ , and the observer position,  $\tilde{O}$ . By rotating the coordinate system from the zenith, sun azimuth system to the coordinate system defined by the observer position, the reflectance angles and sky position can be found easily. Coordinate rotation is also useful for finding the portion of the ergodic cap which reflects the sun light into the path of sight of the observer.

The derivation of the equations for the transformation of rotation of axis expressed in spherical coordinates is given as Appendix A. The angles in the unrotated system are given as unprimed: zenith angle  $\theta$ , azimuth from sun,  $\phi$ . See Fig. 11.

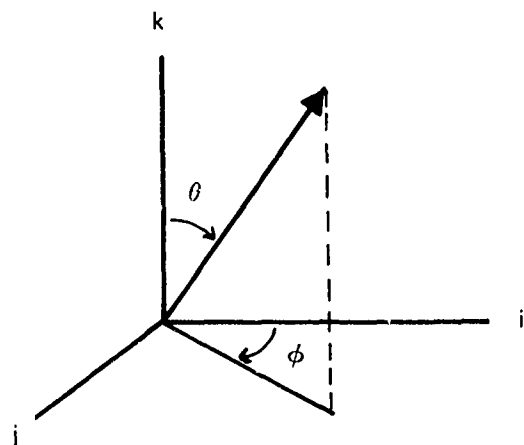


Fig. 11. Unrotated coordinate system.

The rotated coordinate system is defined by angles  $\theta_1$  and  $\phi_1$  in the unrotated system. See Fig. 12.

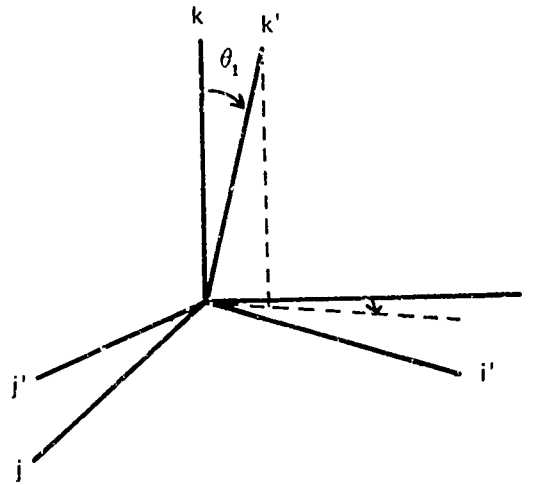


Fig. 12. Rotated axes.

The angles in the rotated system are denoted as primed values,  $\theta'$   $\phi'$ . See Fig. 13.

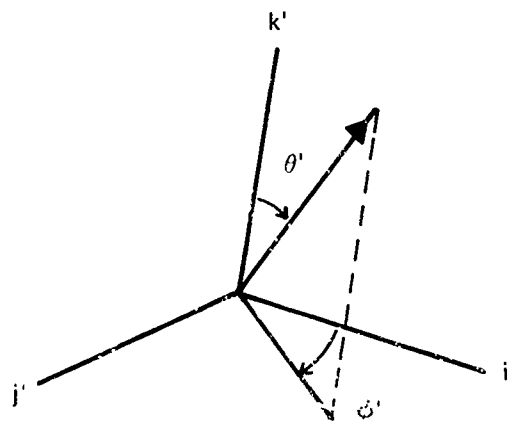


Fig. 13. Rotated coordinate system.

The basic equations for finding direction angles in a rotated system are as follows (equations from Group A.12 in Appendix A).

$$\cos\theta' = \sin\theta \cos\phi \sin\theta_1 \cos\phi_1 + \sin\theta \sin\phi \sin\theta_1 \sin\phi_1 + \cos\theta \cos\theta_1 \quad (3.2.8)$$

$$\cos\phi' = [\sin\theta \cos\phi \sin\theta_1 \cos\phi_1 + \sin\theta \sin\phi \cos\theta_1 \sin\phi_1 - \cos\theta \sin\theta_1] \div \sin\theta' \quad (3.2.9)$$

and

$$\sin\phi' = [-\sin\theta \cos\phi \sin\phi_1 + \sin\theta \sin\phi \cos\phi_1] \div \sin\theta' \quad (3.2.10)$$

Eqs. 3.2.8 through 3.2.10 are for finding the zenith angle  $\theta'$  and azimuth  $\phi'$  in the rotated system for the vector at zenith angle  $\theta$  and azimuth  $\phi$  in the unrotated system. The rotated axes are defined by zenith angle  $\theta_1$  and azimuth  $\phi_1$ . It is necessary to find both  $\sin\phi'$  and  $\cos\phi'$  in order to place  $\phi'$  in the correct quadrant.

The basic equations for finding direction angles in the unrotated system are as follows (equations are from Group A.11 in Appendix A).

$$\cos\theta = -\sin\theta' \cos\phi' \sin\theta_1 + \cos\theta' \cos\theta_1 \quad (3.2.11)$$

$$\cos\phi = [\sin\theta' \cos\phi' \cos\theta_1 \cos\phi_1 - \sin\theta' \sin\phi' \sin\phi_1 + \cos\theta' \sin\theta_1 \cos\phi_1] \div \sin\theta \quad (3.2.12)$$

$$\sin\phi = [\sin\theta' \cos\phi' \cos\theta_1 \sin\phi_1 + \sin\theta' \sin\phi' \cos\phi_1 + \cos\theta' \sin\theta_1 \sin\phi_1] \div \sin\theta \quad (3.2.13)$$

Eqs. 3.2.11 through 3.2.13 are for computing the zenith angle  $\theta$  and azimuth  $\phi$  in the unrotated system for the vector at zenith angle  $\theta'$  and azimuth  $\phi'$  in the rotated system. The rotated axes are again defined by zenith angle  $\theta_1$  and azimuth  $\phi_1$ . Again it is necessary to find both  $\sin\phi$  and  $\cos\phi$  in order to place the azimuth  $\phi$  in the correct quadrant.

### 3.3 Occultation from Light Sources

The ergodic cap simulates the slope characteristics of the wind-ruffled sea, but does not simulate the effect of hiding of one wave by another. A given point on the surface of the sea will sometimes be obscured from a light source; this effect increases as the zenith angle of the light source becomes large.  $Q^\circ(\Psi)$  is the average fractional time that an incident source from elevation angle  $\Psi$  reaches a given point on the sea surface without first having intersected the water surface at some other point. The derivation of  $Q^\circ(\Psi)$  is given in Appendix B by MacAdam, it is consistent with the derivations given in Reference 2.

$$Q^\circ(\Psi) = \exp \left[ - \frac{\sigma}{\tan \Psi \sqrt{2\pi}} \right] \quad (3.3.1)$$

Changing from elevation angle notation to zenith angle notation, and substituting from Eq. 3.1.5 for  $\sigma$ ,



$$Q^{\circ}(\theta) = \exp(-0.0140 \tan \theta \sqrt{v}). \quad (3.3.2)$$

$Q^{\circ}(\theta)$  is the fraction of the light from a source at zenith angle  $\theta$  which reaches the sea surface.

### 3.4 Sun Glitter

The time-averaged sunlight reflected by the water-wave facets is called the sun glitter. The average apparent sun radiance,  $\bar{N}_s(\theta_s, 0)$  is partially hidden from the sea surface by other waves. The radiance that reaches the water is  $\bar{N}_s(\theta_s, 0) Q^{\circ}(\theta_s)$ . This radiance is reflected at angle  $\theta_{SR}$  into the path of sight of the sensor. The proportion of the time this sun radiance will be reflected into the path of sight is  $A_p(\Delta t)/A_p$ .  $A_p$  is the total projected area of the ergodic cap. The equation for  $A_p$  will be derived in the next section which will concern the sky reflectance for the wind-ruffled sea

$$\bar{N}_g(\theta_p, \phi_p) = \bar{N}_s(\theta_s, 0) Q^{\circ}(\theta_s) r(\theta_{SR}) A_p(\Delta t)/A_p \quad (3.4.1)$$

The photometric equation is directly analogous.

$$\bar{B}_g(\theta_p, \phi_p) = \bar{B}_s(\theta_s, 0) Q^{\circ}(\theta_s) r(\theta_{SR}) A_p(\Delta t)/A_p \quad (3.4.2)$$

$A_p(\Delta t)$  is the portion of the projected ergodic cap that is tilted at the appropriate angles to reflect the sun into the path of sight. Thus,

$$A_p(\Delta t) = \frac{V(\Delta t) \cos \theta_{SR}}{\cos \theta_{SN}} \quad (3.4.3)$$

where  $V(\Delta t)$  is the probability of the wave slopes which reflect the sun into the path of sight,  $\theta_{SR}$  is the angle between the observer and the normal from the facet reflecting the center of the sun, and  $\theta_{SN}$  is the zenith angle of the normal from the facet reflecting the center of the sun, the probability  $V(\Delta t)$  will be derived first, and then the equations for computing the angles  $\theta_{SR}$  and  $\theta_{SN}$  will be set forth.

The first step in deriving the probability will be to redraw the probability function from Fig. 9 by changing variables, see Fig. 14. The radius changes from  $X$  to  $\tan \theta$  and the height  $y$  becomes  $y'$  and is

$$y' = \frac{1}{2\pi\sigma^2} \exp\left(-\frac{\tan^2 \theta}{2\sigma^2}\right) \quad (3.4.4)$$

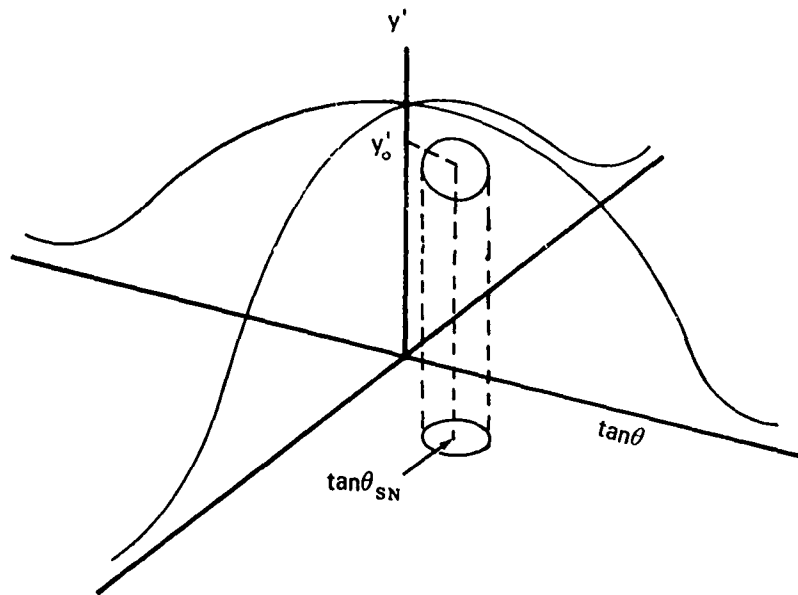


Fig. 14. Distribution of wave slopes.

$$V = \frac{1}{\sigma^2} \int_0^\infty \tan \theta \exp \left( -\frac{\tan^2 \theta}{2\sigma^2} \right) d \tan \theta \quad (3.4.5)$$

$$= \frac{1}{\sigma^2} \left[ -\frac{2\sigma^2}{2} \exp \left( -\frac{\tan^2 \theta}{2\sigma^2} \right) \right]_0^\infty = 1 \quad (3.4.6)$$

The element of volume of the probability function representing the wave slopes which reflect the solar disk of size  $\Omega_s$ , can reasonably be represented as an elliptical cylinder. The center of the cylinder is at  $\tan \theta_{SN}$ , the slope which reflects the center of the sun. The height of the cylinder is  $y'_0$  where

$$y'_0 = \frac{1}{2\pi\sigma^2} \exp \left( -\frac{\tan^2 \theta_{SN}}{2\sigma^2} \right). \quad (3.4.7)$$

The ellipse of the cylinder is the tolerance ellipse as defined by Cox and Munk Ref. 14. Its area  $\Delta t$  is given as

$$\Delta t = \frac{1}{4} \pi \epsilon^2 \sec^3 \beta_0 \sec \omega_0 \quad (3.4.8)$$

where  $\epsilon$  is the angular radius of the sun in radians,  $\beta_0$  is the tilt angle and is equivalent to the angle  $\theta_{SN}$  in the notation herein, and  $\omega_0$  is the angle of reflection used herein as  $\theta_{SR}$ . Thus Eq. 3.4.8 can be rewritten,

$$\Delta t = \frac{1}{4} \pi \epsilon^2 \sec^3 \theta_{SN} \sec \theta_{SR} \quad (3.4.9)$$

The angular radius of the sun for mean solar distance is

$$\epsilon = 0.004659 \text{ radians} \quad (3.4.10)$$

The volume of an elliptical cylinder is the height times the area of the ellipse. Thus combining Eqs. 3.4.7 and 3.4.9,

$$V(\Delta t) = \frac{\epsilon^2 \sec^3 \theta_{SN} \sec \theta_{SR}}{8\sigma^2} \exp\left(-\frac{\tan^2 \theta_{SN}}{2\sigma^2}\right). \quad (3.4.11)$$

Finally combining Eqs. 3.4.3 and 3.4.11, the projected area of the ergodic cap which reflects the sun into the path of sight is,

$$A_p(\Delta t) = \frac{\epsilon^2 \exp\left(-\frac{\tan^2 \theta_{SN}}{2\sigma^2}\right)}{8\sigma^2 \cos^4 \theta_{SN}} \quad (3.4.12)$$

Substituting for  $\sigma^2$  from Eq. 3.1.4,

$$A_p(\Delta t) = \frac{\epsilon^2 \exp\left(-\frac{\tan^2 \theta_{SN}}{0.00246v}\right)}{0.00984v \cos^4 \theta_{SN}} \quad (3.4.13)$$

The angles  $\theta_{SR}$  and  $\theta_{SN}$  are easily computed by rotating from one coordinate system to another and back again. The principal or unrotated coordinate system is defined by the true zenith, and the azimuth from the sun. The prime coordinate system is defined by a vector  $\tilde{S}$  toward the sun at  $\theta_s$  and  $\phi_s = 0$ . See Fig. 15.

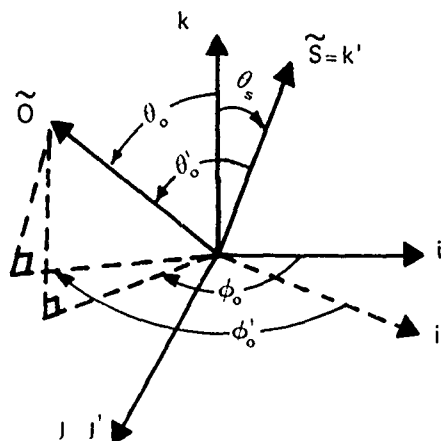


Fig. 15. Observer O vector in principal and prime coordinate systems.

The observer's position vector has a zenith angle  $\theta_o$  and azimuth  $\phi_o$ . The relationship of the observer angles  $\theta_o$ ,  $\phi_o$  to the path of sight angles was discussed in section 2.3. The observer's position in the rotated system is found by appropriate substitution into Eqs. 3.2.8 and 3.2.9. Since  $\phi_1 = \phi_s = 0$ , some of the terms drop out.

$$\cos\theta'_o = \sin\theta_o \cos\phi_o \sin\theta_s + \cos\theta_o \cos\theta_s \quad (3.4.14)$$

$$\cos\phi'_o = [\sin\theta_o \cos\phi_o \cos\theta_s - \cos\theta_o \sin\theta_s] \div \sin\theta'_o \quad (3.4.15)$$

It is not necessary in this case to determine  $\phi'_o$  directly only  $\cos\phi'_o$ , the reason for this will be seen shortly. Therefore, it is not necessary to compute  $\sin\phi'_o$  from Eq. 3.2.10. Since  $\theta'_o$  is the angle between the sun  $\tilde{S}$  and the observer  $\tilde{O}$ , the Fresnel reflectance angle,  $\theta_{SR}$ , is equal to half of  $\theta'_o$ .

$$\theta_{SR} = \frac{\theta'_o}{2} \quad (3.4.16)$$

The normal from the facet reflecting the center of the sun  $\tilde{SN}$  is at  $\theta'_o/2$ ,  $\phi'_o$  in the prime coordinate system, see Fig. 16.

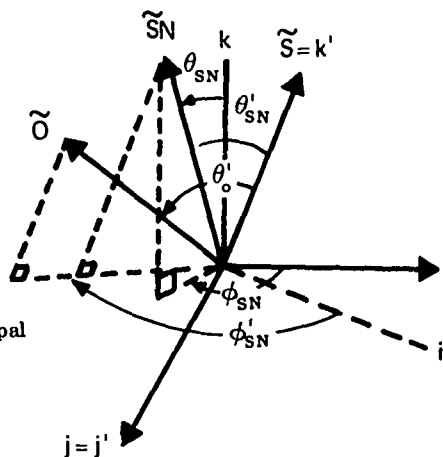


Fig. 16. Normal,  $\tilde{SN}$ , reflecting the sun in principal and prime coordinate systems.

Rotating back to the principal coordinate system by substituting appropriately in Eq. 3.2.11, Eq. 3.4.17 is obtained.

$$\cos\theta_{SN} = -\sin\frac{\theta'_o}{2} \cos\phi'_o \sin\theta_s + \cos\frac{\theta'_o}{2} \cos\theta_s \quad (3.4.17)$$

### 3.5 Sky Reflectance

The time-averaged wind-ruffled sea reflects light from various portions of the sky. To simplify the calculation, the curved surface of the ergodic cap is represented by a series of flat surfaces. Thus, the time-averaged inherent radiance of the sea due to sky reflectance can be calculated by summing the appropriately weighted reflected sky radiances by each of the flat surfaces.

$$\bar{N}_{sky}(\theta_P, \phi_P) = \frac{1}{A_P} \left\{ \sum_{i=1}^n \left[ \sum_{j=1}^m N(\theta_{B_i}, \phi_{B_i})_{ij} Q^\circ(\theta_{B_ij}) r(\theta_{B_{Rij}}) \cos \theta_{B_{Rij}} \right] \frac{A_H(\theta_{N1})}{\cos \theta_{N1}} \right\} \quad (3.5.1)$$

The equation is similar for the photopic case.

The surface of the ergodic cap can be cut into sections represented by flat surfaces. Each flat surface is represented by a normal from the surface at  $\theta_N$  and  $\phi_N$  where  $\theta_N = (\theta_1 + \theta_2)/2$  and  $\phi_N = (\phi_1 + \phi_2)/2$ ;  $\Delta\theta_N = \theta_2 - \theta_1$  and  $\Delta\phi_N = \phi_2 - \phi_1$ . The slopes from  $\theta_N = 0^\circ$  to  $\Delta\theta/2$  regardless of azimuth are represented by a horizontal surface,  $\theta_N = 0$ . Thus, from Eqs. 3.2.2 and 3.2.3

$$A_H(0) = -\exp\left(-\frac{\tan^2(\Delta\theta_N/2)}{2\sigma^2}\right) + 1 \quad (3.5.2)$$

and from Eqs. 3.2.4 and 3.2.5

$$A_H(\theta_N) = \frac{1}{m} \left[ -\exp\left(-\frac{\tan^2(\theta_N + \Delta\theta_N/2)}{2\sigma^2}\right) + \exp\left(-\frac{\tan^2(\theta_N - \Delta\theta_N/2)}{2\sigma^2}\right) \right] \quad (3.5.3)$$

The term  $1/m = \Delta\phi/2\pi$  where  $\Delta\phi$  is in radians. The number  $n$  of  $i$  or  $\theta_N$  terms depends upon wind speed and the assigned precision level for the total wave slope probability. The number of  $\theta_N$  terms for an ergodic cap with  $\Delta\theta_N = 5^\circ$ , with slopes greater than  $\theta_{Nn} + 5^\circ$  contributing less than  $10^{-4}$  to the total wave slope probability is given in Table 3 for various wind speeds.

Table 3. Ergodic cap specifications for  $\Delta\theta_N = 5^\circ$ .

	Wind speed (knots)								
	0	2	4	8	14	20	26	32	38
$n$	1	3	4	6	7	8	9	9	10
$\theta_{Nn}$ (degrees)	0	10	15	25	30	35	40	40	45

The three terms  $\cos\theta_{BR} A_H(\theta_N)/\cos\theta_N$  are actually the projected area of each flat surface or element of the ergodic cap

$$A_P(\theta_N) = \frac{\cos\theta_{BR} A_H(\theta_N)}{\cos\theta_N} \quad (3.5.4)$$

Thus, the total projected area is the sum of all these elemental projected areas.

$$A_P = \sum_{i=1}^n \left[ \sum_{j=1}^m \cos\theta_{B_{Rij}} \right] \frac{A_H(\theta_N)_i}{\cos\theta_{N1}} \quad (3.5.5)$$

The total projected area is within 1 percent of the cosine of the observer angle,  $A_p = \cos\theta_o$ , for observer zenith angles 0 to 70°. For larger observer zenith angles the projected area becomes a function of wind speed. Evaluation of the projected area for large observer zenith angles for an ergodic cap with flat surfaces representing  $\Delta\theta_N = 5^\circ$  and  $\Delta\phi_N = 10^\circ$ , is given in Table 4.

Table 4. Total projected area,  $A_p$ , of ergodic cap for large observer zenith angles.

Observer Zenith Angle $\theta_0$	Wind Speed (Knots)								
	0	2	4	8	14	20	26	32	38
75	0.259	0.259	0.259	0.259	0.260	0.262	0.264	0.267	0.270
80	0.174	0.174	0.174	0.175	0.179	0.184	0.189	0.194	0.199
85	0.0872	0.0878	0.0907	0.0977	0.107	0.116	0.124	0.131	0.137
90	0.00000	0.0198	0.0282	0.0398	0.0527	0.0630	0.0718	0.0796	0.0868

The reflectance angle  $\theta_{BR}$  and the sky position angles  $\theta_B, \phi_B$ , can be computed by assuming unit vector notation and rotating axes. The observer position vector  $\vec{O}$  at  $\theta_o, \phi_o$  defines the rotated system. The normal  $\vec{N}$  from a given ergodic cap element is at  $\theta_N, \phi_N$ . The first task is to find the normal direction angles,  $\theta'_N, \phi'_N$ , in the rotated system. Appropriately substituting into Eqs. 3.2.8, 3.2.9, and 3.2.10.

$$\cos\theta'_N = \sin\theta_N \cos\phi_N \sin\theta_o \cos\phi_o + \sin\theta_N \sin\phi_N \sin\theta_o \sin\phi_o + \cos\theta_N \cos\theta_o \quad (3.5.6)$$

$$\cos\phi'_N = [\sin\theta_N \cos\phi_N \cos\theta_o \cos\phi_o + \sin\theta_N \sin\phi_N \cos\theta_o \sin\phi_o - \cos\theta_N \sin\theta_o] \div \sin\theta'_N \quad (3.5.7)$$

$$\sin\phi'_N = [-\sin\theta_N \cos\phi_N \sin\phi_o + \sin\theta_N \sin\phi_N \cos\phi_o] \div \sin\theta'_N \quad (3.5.8)$$

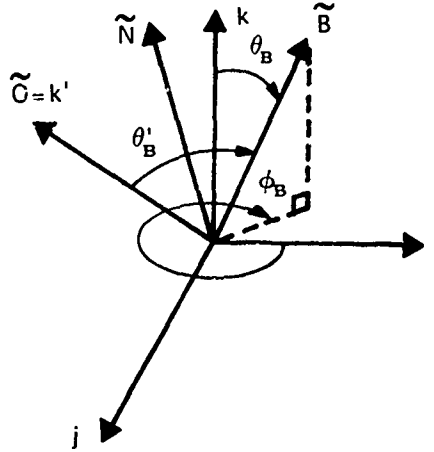
$\theta'_N$  is also the Fresnel reflectance angle,  $\theta_{BR}$ . When  $\theta'_N = \theta_{BR} \geq 90^\circ$ , the reflectance is zero and the projected area is zero. The sky position in the rotated system is twice the Fresnel reflectance angle and in the same azimuth as the normal from the reflecting surface. Thus

$$\theta'_B = 2\theta'_N \quad (3.5.9)$$

$$\phi'_B = \phi'_N \quad (3.5.10)$$

The sky position in the unrotated system is determined by appropriately substituting into Eqs. 3.2.11 through 3.2.13. See Fig. 17.

Fig. 17. Sky position vector  $\tilde{B}$  in prime and principal system.



$$\cos\theta_B = \sin\theta'_B \cos\phi'_B \sin\theta_0 + \cos\theta'_B \cos\theta_0 \quad (3.5.11)$$

$$\cos\phi_B = [\sin\theta'_B \cos\phi'_B \cos\theta_0 \cos\phi_0 - \sin\theta'_B \sin\phi'_B \sin\phi_0 + \cos\theta'_B \sin\theta_0 \cos\phi_0] \div \sin\theta_B \quad (3.5.12)$$

$$\sin\phi_B = [\sin\theta'_B \cos\phi'_B \cos\theta_0 \sin\phi_0 + \sin\theta'_B \sin\phi'_B \cos\phi_0 + \cos\theta'_B \sin\theta_0 \sin\phi_0] \div \sin\theta_B \quad (3.5.13)$$

When  $\theta_B > 90^\circ$ , the sky radiance (luminance) is considered = zero since the contribution from the lower sky (sea surface) is negligible. Also, when the sky luminance distribution is symmetrical with respect to the azimuth of the sun (clear days without clouds are reasonably symmetrical) it is not necessary to compute  $\sin\phi_B$ ;  $\cos\phi_B$  will yield answers between 0 and  $180^\circ$  in azimuth.

### 3.6 Upwelling Light

The light upwelling from the surface of the wind-ruffled sea is similar in form to the light upwelling from a calm sea, (see Eqs. 2.4.23 and 2.4.36), with these differences: Each source radiance,  $N(\theta_B, \phi_B)$ , will be accompanied by an occultation term,  $Q^\circ(\theta_B)$ , and a time-averaged transmittance and cosine,  $\int t(\theta_B) \cos\theta_B d\hat{t}$  for the transmittance and redirection of the light ray beneath the surface of the sea by the tilted wave facets. The internal reflectance of the water  $r_s$  will be a time-averaged internal reflectance of diffuse light  $\int r_s d\hat{t}$ . Finally, the transmittance of the diffuse light upward in the direction of the path of sight is a time-averaged transmittance  $\int t(\theta) d\hat{t}$ . Thus,

$$\begin{aligned} \bar{N}_u(\theta_p, \phi_p) = & \left[ \int_{2\pi} N(\theta_B, \phi_B) Q^\circ(\theta_B) \int t(\theta_B) \cos\theta_B d\hat{t} d\Omega_B \right. \\ & \left. + \bar{N}_s(\theta_s, 0) Q^\circ(\theta_s) \int t(\theta_s) \cos\theta_s d\hat{t} d\Omega_s \right] \times \\ & \left[ \frac{R_\infty}{\pi(1-R_\infty \int r_s d\hat{t})} \int t(\theta_0) d\hat{t} \left( \frac{n}{n'} \right)^2 \right] \end{aligned} \quad (3.6.1)$$

The photometric equation will not be written out since it is necessary only to substitute the luminance symbol, B, for every radiance symbol, N.

### 3.6.1 TIME-AVERAGED TRANSMITTANCE AND COSINE

The slope distribution of the wind-ruffled sea surface is represented by an ergodic cap with flat elements as was described in the preceding section on sky reflectance. For a single source at angle  $\theta_B$ , the occultation is invariant but the Fresnel transmittance angle,  $\theta_{BR}$ , is different for each flat element of the ergodic cap. Second, the ratio of the solid angles and projected areas changes with each element,  $(ds \cos \theta_{BR} d\Omega) \div (ds \cos \theta_{BR} d\Omega')$  [see Eq. 2.4.1]. Third, a flat plate collector will receive the radiance at the refracted angle  $\theta_B$  and solid angle  $d\Omega'$  which will be different for each element of the ergodic cap. Fourth, the probability of transmitting the radiance from  $\tilde{B}$  by the elemental surface area represented by the ergodic cap is  $\cos \theta_{BR} A_H(\theta_N)/A_p \cos \theta_N$ . Thus, for one element of the ergodic cap, the irradiance beneath the surface of the water,  $\Delta H(0,0)$ , received from the source radiance at  $\theta_B, \phi_B$  is

$$\Delta H(0,0) = \frac{1}{A_p} \left[ N(\theta_B, \phi_B) Q^o(\theta_B) t(\theta_{BR}) \frac{ds \cos \theta_{BR} d\Omega}{ds \cos \theta_{BR} d\Omega'} \cos \theta_B d\Omega' \cos \theta_{BR} \frac{A_H(\theta_N)}{\cos \theta_N} \right] \quad (3.6.2)$$

The irradiance received from the source radiance through all elements of the ergodic cap is, as follows,

$$H(0,0) = N(\theta_B, \phi_B) Q^o(\theta_B) \left\{ \frac{\sum_{i=1}^n \left( \sum_{j=1}^m t(\theta_{BRij}) \frac{\cos^2 \theta_{BRij}}{\cos \theta_{BRij}} \cos \theta_{Bij} \right) \frac{A_H(\theta_{Ni})}{\cos \theta_{Ni}}}{\sum_{i=1}^n \left( \sum_{j=1}^m \cos \theta_{BRij} \right) \frac{A_H(\theta_{Ni})}{\cos \theta_{Ni}}} \right\} d\Omega_B \quad (3.6.3)$$

The term in braces is called the time-averaged transmittance and cosine,  $\int t(\theta) \cos \theta d\hat{t}$ .

$$\int t(\theta_B) \cos \theta_B d\hat{t} = \frac{\sum_{i=1}^n \left[ \sum_{j=1}^m t(\theta_{BRij}) \frac{\cos^2 \theta_{BRij}}{\cos \theta_{BRij}} \cos \theta_{Bij} \right] \frac{A_H(\theta_{Ni})}{\cos \theta_{Ni}}}{\sum_{i=1}^n \left[ \sum_{j=1}^m \cos \theta_{BRij} \right] \frac{A_H(\theta_{Ni})}{\cos \theta_{Ni}}} \quad (3.6.4)$$



Thus, the irradiance received from the source radiance at  $\theta_B$  is

$$H(0,0) = N(\theta_B, \phi_B) Q^0(\theta_B) \int t(\theta_B) \cos \theta_B d\hat{t} d\Omega_B \quad (3.6.5)$$

and the irradiance from the upper hemisphere is

$$H(0,0) = \int_{2\pi} N(\theta_B, \phi_B) Q^0(\theta_B) \int t(\theta_B) \cos \theta_B d\hat{t} d\Omega_B \quad (3.6.6)$$

The Fresnel transmittance angle  $\theta_{BR}$  is the angle between a vector in the source direction,  $\tilde{B}$  and the normal from the flat surface,  $\tilde{N}$ . The axes are rotated to the vector  $\tilde{N}$  and the luminance zenith angle,  $\theta_B$ , determined in the prime system.  $\theta'_B = \theta_{BR}$ . See Fig. 18.

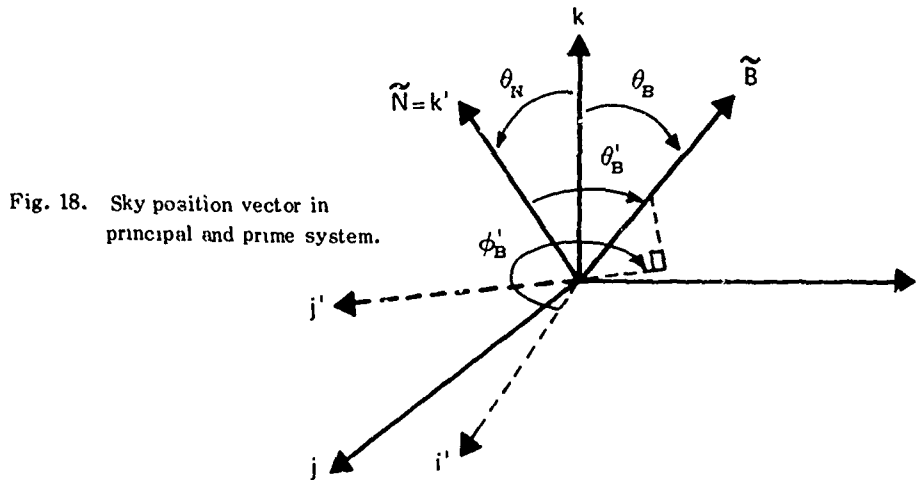


Fig. 18. Sky position vector in principal and prime system.

Since the time-averaged transmittance and cosine should not change with source azimuth, the integral in Eq. 3.6.4 can be evaluated by assuming  $\phi_B = 0$ . Thus, from Eq. 3.2.8,

$$\cos \theta_{BR} = \sin \theta_B \sin \theta_N \cos \phi_N + \cos \theta_B \cos \theta_N \quad (3.6.7)$$

When  $\theta_{BR} \geq 90^\circ$  both the transmittance and the projected area of the element are zero and that element of the ergodic cap is not included in the summation. The refracted angle  $\theta_{BR}$  is found by means of Snell's law, Eq. 2.1.1,

$$\theta_{BR} = \sin^{-1} \left( \frac{n}{n'} \sin \theta_{BR} \right) \quad (3.6.8)$$

The zenith angle of the refracted ray  $\Theta_B$  can be found by noting the analogy between the angles beneath the surface of the water and above the surface of the water. A new vector  $\tilde{B}$  is defined in the opposite direction to the refracted ray, see Fig. 19.

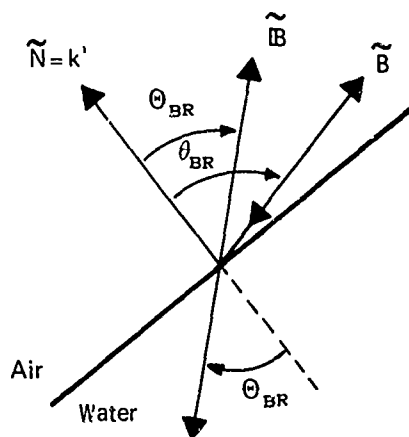


Fig. 19. Plane passed through  $\tilde{N}$  and  $\tilde{B}$ .

$\phi'_B$  is the azimuth of both the radiance vector  $\tilde{B}$  and the refracted vector  $\tilde{B}$  in the prime system defined by the normal  $\tilde{N}$ . The zenith angle of the refracted vector in the prime system  $\Theta'_B = \Theta_{BR}$ .  $\cos\phi'_B$  is found by appropriate substitution into Eq. 3.2.9.

$$\cos\phi'_B = \left[ \sin\theta_B \cos\theta_N \cos\phi_N - \cos\theta_B \sin\theta_N \right] \div \sin\theta_{BR} \quad (3.6.9)$$

Now the zenith angle of the refracted ray  $\Theta_B$  can be found by rotating from the prime system to the principal system by using Eq. 3.2.11 appropriately.

$$\cos\Theta_B = -\sin\Theta'_B \cos\phi'_B \sin\theta_N + \cos\Theta'_B \cos\theta_N \quad (3.6.10)$$

The time-averaged transmittance and cosine was evaluated for various source radiance angles and wind speeds for an index of refraction  $n' = 1.341$  (photopic, sea water) with an ergodic cap element size of  $\Delta\theta = 5^\circ$  and  $\Delta\phi = 10^\circ$ . The result is given in Table 5. These values may also be used for other wavelengths in the visible spectrum for both salt water or fresh water if the accuracy desired is no greater than 1 percent.

Table 5. Time-averaged transmittance and cosine for source at zenith angle, theta.

Source Zenith Angle	Wind Speed (Knots)								
	0	2	4	8	14	20	26	32	38
0	0.979	0.977	0.976	0.974	0.970	0.967	0.963	0.960	0.956
5	0.975	0.974	0.972	0.970	0.966	0.963	0.959	0.956	0.952
10	0.964	0.962	0.961	0.959	0.955	0.951	0.948	0.944	0.941
15	0.945	0.944	0.943	0.940	0.936	0.933	0.929	0.926	0.922
20	0.920	0.918	0.917	0.914	0.910	0.907	0.903	0.899	0.896
25	0.887	0.885	0.884	0.881	0.877	0.873	0.870	0.866	0.863
30	0.847	0.845	0.844	0.841	0.837	0.833	0.829	0.826	0.822
35	0.800	0.798	0.797	0.794	0.790	0.786	0.782	0.779	0.775
40	0.747	0.745	0.743	0.741	0.736	0.733	0.729	0.725	0.722
45	0.687	0.685	0.684	0.681	0.677	0.673	0.669	0.666	0.663
50	0.620	0.619	0.617	0.615	0.611	0.608	0.605	0.602	0.599
55	0.548	0.546	0.545	0.543	0.540	0.538	0.536	0.534	0.532
60	0.469	0.468	0.468	0.466	0.465	0.464	0.464	0.464	0.463
65	0.385	0.385	0.385	0.386	0.387	0.389	0.391	0.393	0.395
70	0.295	0.298	0.299	0.303	0.310	0.315	0.321	0.325	0.329
75	0.203	0.209	0.214	0.224	0.236	0.247	0.255	0.262	0.268
80	0.113	0.126	0.136	0.153	0.172	0.186	0.197	0.206	0.213
85	0.0361	0.0610	0.0751	0.0969	0.119	0.135	0.148	0.157	0.165
90	0	0.0265	0.0390	0.0594	0.0809	0.0961	0.108	0.117	0.124

### 3.6.2 TIME-AVERAGED INTERNAL REFLECTANCE OF DIFFUSE LIGHT

For a wind-ruffled sea, the equation for the internal reflectance of diffuse light, Eq. 2.4.14, changes in the following manner

$$\int r_s d\hat{t} = \frac{1}{\pi} \int_{2\pi} \left[ \int r(\Theta) d\hat{t} \right] \cos\Theta d\Omega'. \quad (3.6.11)$$

The term in the brackets is the time-averaged internal reflectance of diffuse light into the path of sight  $\Theta$  of a sensor. See Fig. 20.

$$\int r(\Theta) d\hat{t} = \frac{1}{A_p} \left\{ \sum_{i=1}^n \left[ \sum_{j=1}^m r(\Theta_{R_{ij}}) \cos\Theta_{R_{ij}} \right] \frac{A_H(\Theta_{N_i})}{\cos\Theta_{N_i}} \right\} \quad (3.6.12)$$

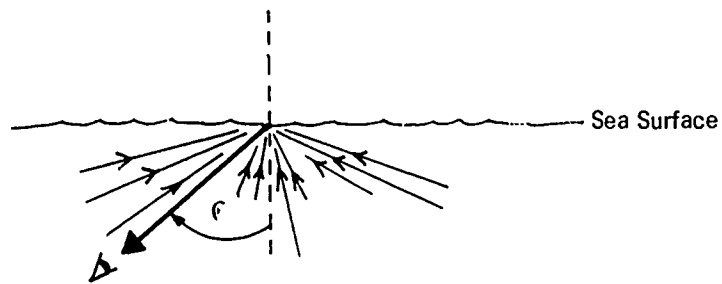


Fig. 20. Time-averaged internal reflectance of diffuse light.

For this computation the ergodic cap is assumed to have a normal  $N'$  from beneath the surface at a nadir angle  $\Theta_N$ , and azimuth,  $\Phi_N$  where in this instance  $\theta_N = \Theta_N$  and  $\Phi_N = \phi_N + 180^\circ$ . See Fig. 21.

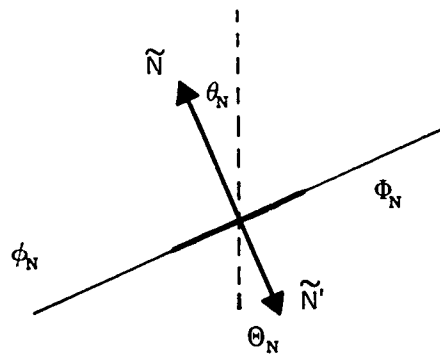


Fig. 21. Element of ergodic cap.

Since the time-averaged reflectance should not change with sensor azimuth,  $\Phi_o$  is assumed equal to zero. The reflectance angle  $\Theta_R$  is found by appropriate substitution into Eq. 3.2.8.

$$\cos\Theta_R = \sin\Theta_N \cos\Phi_N \sin\Theta_o + \cos\Theta_N \cos\Theta_o \quad (3.6.13)$$

The angle  $\theta_R$  is found from Snell's law, rephrasing Eq. 2.1.1,

$$\theta_R = \sin^{-1} \left( \frac{n'}{n} \sin\Theta \right) \quad (3.6.14)$$

The Fresnel reflectance  $r(\theta_R)$  is found directly from Eq. 2.1.2  $r(\theta_R) = r(\theta_R)$ . The total projected area of the ergodic cap is the same as before, or rephrased in terms of nadir angles

$$A_p = \sum_{i=1}^n \left[ \sum_{j=1}^m \cos \theta_{Rij} \right] \frac{A_H(\theta_{Ni})}{\cos \theta_{Ni}} \quad (3.6.15)$$

The time-averaged internal reflectance for diffuse light was evaluated for an index of refraction  $n' = 1.341$  (photopic sea water) with an ergodic cap element size of  $\Delta \theta = 5^\circ$ ,  $\Delta \phi = 10^\circ$ . The summative grid for Eq. 3.6.12 was the same. The result is given in Table 6 for wind speeds 0 to 38 knots. These values may be used for fresh water as well as salt water, for all wavelengths in the visible spectrum with an accuracy of 2 percent.

Table 6. Time-averaged internal reflectance of diffuse light for  $n' = 1.341$

		Wind Speed (Knots)								
		0	2	4	8	14	20	26	32	38
$\int r_s d\hat{t}$		0.485	0.482	0.481	0.478	0.474	0.470	0.466	0.463	0.459

### 3.6.3 TIME-AVERAGED TRANSMITTANCE

The time-averaged Fresnel transmittance toward  $\theta_o$  of a uniform radiance (luminance) from beneath the surface of the water is equivalent to the time-averaged transmittance from air-to-water from a source at  $\theta_o$ . For ease in computation let  $\theta_B = \theta_o$ . Then, the time-averaged transmittance is the sum of the transmittances of each of the elements of the ergodic cap weighted by the probability appropriate to the source direction  $\theta_B$ .

$$\int t(\theta_B) d\hat{t} = \frac{1}{A_p} \left\{ \sum_{i=1}^n \left[ \sum_{j=1}^m t(\theta_{Brij}) \cos \theta_{Brij} \right] \frac{A_H(\theta_{Ni})}{\cos \theta_{Ni}} \right\} \quad (3.6.16)$$

$A_p$  is the projected area as defined in Eq. 3.5.6. Since the time-averaged transmittance should not change with source azimuth, the integral is evaluated by assuming  $\phi_B = 0$ . Thus  $\theta_{BR}$  can be found from Eq. 3.6.7.

The time-averaged transmittance has been evaluated for the index of refraction  $n' = 1.341$  (photopic index for sea water). The ergodic cap was again made up of flat surfaces representing  $\Delta\theta_N = 5^\circ$  and  $\Delta\phi_N = 10^\circ$ . The results showed the time-averaged transmittance to be equal to the Fresnel transmittance within 1 percent,  $\int t(\theta) d\hat{t} = t(\theta)$ , for source zenith angles  $0^\circ$  to  $65^\circ$ . The values for zenith angles greater than  $65^\circ$  are given in Table 7. The slight decrease and then increase with wind speed at zenith angle  $70^\circ$  is consistent with the results for the smaller zenith angles. For zenith angles  $0^\circ$  to  $60^\circ$ , the time-averaged transmittance consistently decreased with increasing wind speed 0 to 38 knots, even though the decrease was less than 1 percent between 0 and 38 knots. The values in Table 7 may be used for all wavelengths in the visible spectrum for both salt water and fresh water if the desired accuracy is no greater than 1 percent.

Table 7. Time-averaged transmittance for  $n' = 1.341$  for source at zenith angle theta.

Zenith Angle $\theta$ Degrees	Wind Speed (Knots)								
	0	2	4	8	14	20	26	32	38
70	0.864	0.864	0.863	0.863	0.865	0.868	0.872	0.875	0.879
75	0.785	0.787	0.790	0.797	0.809	0.820	0.830	0.838	0.845
80	0.649	0.666	0.680	0.708	0.739	0.763	0.781	0.795	0.807
85	0.414	0.499	0.542	0.603	0.660	0.698	0.726	0.747	0.765
90	0.0000	0.359	0.419	0.506	0.585	0.636	0.672	0.699	0.722

### 3.7 Directional Radiance (Luminance) of the Time-Averaged Wind-ruffled Sea

The directional radiance (luminance) of the wind-blown sea due to time- or space- averaged small capillary waves is the sum of the terms for sun glitter, sky reflectance, and upwelling light. In radiometric form,

$$\bar{N}(\theta_p, \phi_p) = \bar{N}_s(\theta_p, \phi_p) + \bar{N}_{sky}(\theta_p) + \bar{N}_u(\theta_p, \phi_p). \quad (3.7.1)$$

The photometric form is the same.

## 4. RADIANCE (LUMINANCE) PATTERNS OF LARGE WAVES

Photographs of the sea surface usually contain radiance patterns which indicate that the radiances are not time- or space-averaged. The photographic work by Cox and Munk (Ref. 15) to obtain the slope distribution utilized a defocused camera in order to obtain photographs of averaged radiances. The resolution

of many photographs is such that the radiance pattern indicates the larger wave train pattern. The small capillary waves however are normally not resolved and can be assumed to be time- or space-averaged. The calculation methods described in the previous sections can be easily modified to give a reasonable approximation of the intermediate resolution obtained photographically. This is done by tipping the ergodic cap in the direction of the normal from the surface of the large wave. The surface normal used should represent the average slope for the resolution of the photograph, such as 1 ft., 2 ft., 4 ft., etc.

The equations in this fourth section will be stated in radiometric terms. The photometric equations are directly equivalent.

#### 4.1 Tipped Ergodic Cap

For a calculation of intermediate resolution of the time- and/or space-averaged slope distribution of the sea surface, it is desirable to have the capillary or small facet wave distribution separated from the larger, gravity wave component. The capillary distribution probably is partially dependent upon position on the wave train, at or near the peak of the gravity wave the distribution would probably have a larger standard deviation than down in the trough. No such statistics being available, however, it is probably not unreasonable to assume that the wave slope distribution as measured by Cox and Munk is primarily the capillary distribution and for a first approximation, can be assumed to be the same for all positions on the larger waves, the primary effect being that of tipping the distribution according to the slope of the large wave.

Various assumptions may be made about the point-to-point slope distribution of the larger waves. The simplest and least accurate is that of assuming trochoidal shaped waves in the direction of the local wind and of superimposing trochoidal shaped swell from other directions, to represent swell from distant storms. This method is fully described in Reference 3. A more sophisticated method would be to represent the sea surface by Lagrangian equations.<sup>16</sup>

In tipping the ergodic cap in the direction of the normal from the larger wave surface, the vector representing the normal from the wave will be designated as  $\tilde{T}$  with the zenith angle being  $\theta_T$  and the azimuth from the sun being  $\phi_T$ . See Fig. 22.

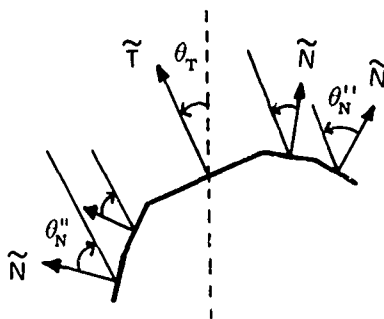


Fig. 22. The tilted ergodic cap.

The vector  $\tilde{T}$  will define a rotated system designated by double primes. The normals from the elements of the ergodic cap  $\tilde{N}$  will be designated by angles  $\theta_N''$  and  $\phi_N''$  which are angles in the double prime system [equivalent to angles in the unrotated system when  $\theta_T, \phi_T$  both = 0, when the cap is untipped]. The horizontal projected area of the element representing the probability of occurrence of slope is in the double prime system and is designated by  $A_H(\theta_N'')$ . The true area is

$$A_T(\theta_N'') = \frac{A_H(\theta_N'')}{\cos \theta_N''} \quad (4.1.1)$$

## 4.2 Sun Glitter

The sunlight reflected from a wave tilted at  $\theta_T, \phi_T$  is found by equations similar to those in Section 3.4. Eq. (3.4.1) for  $\bar{N}_g(\theta_p, \phi_p)$  can be used directly but the equation for the projected portion of the ergodic cap reflecting the sun,  $A_p(\Delta t)$  changes from Eq. 3.4.12 to

$$A_p(\Delta t) = \frac{\epsilon^2 \exp - \frac{\tan^2 \theta_{SN}''}{2\sigma^2}}{8\sigma^2 \cos^4 \theta_{SN}''} \quad (4.2.1)$$

The modified equation for the total projected area of the cap,  $A_p$ , will be given in the next section.

The Fresnel reflectance angle  $\theta_{SR}$  is found in the same manner as for an untipped cap through the use of Eqs. (3.4.14) and (3.4.16). In order to obtain the normal from the cap surface reflecting the center of the sun in the double prime system,  $\theta_{SN}''$ , it is first necessary to obtain the normal position in the unrotated system,  $\theta_{SN}$  and  $\phi_{SN}$ .  $\theta_{SN}$  can again be found through the use of Eqs. (3.4.14) through (3.4.17). In order to find  $\phi_{SN}$ , however, it will be necessary to also compute  $\sin \phi_0'$  by appropriately substituting into Eq. 3.2.10. As before the prime system is defined by the vector  $\tilde{S}$ . Since  $\phi_1 = \phi_s = 0$ , some of the terms drop out.

$$\sin \phi_0' = [\sin \theta_0 \sin \phi_0] + \sin \theta_0' \quad (4.2.2)$$

Then  $\phi_{SN}$  can be found by rotating back to the principal coordinate system and appropriately substituting into Eqs. 3.2.12 and 3.2.13.



$$\cos\phi_{SN} = \left[ \sin\frac{\theta'_0}{2} \cos\phi'_0 \cos\theta'_s + \cos\frac{\theta'_0}{2} \sin\theta'_s \right] \div \sin\theta_{SN} \quad (4.2.3)$$

$$\sin\phi_{SN} = \left[ \sin\frac{\theta'_0}{2} \sin\phi'_0 \right] \div \sin\theta_{SN} \quad (4.2.4)$$

Now rotating to the double prime system defined by the vector  $\tilde{T}$  at  $\theta_T, \phi_T$ , and substituting into Eq. 3.2.8,  $\theta''_{SN}$  is obtained. See Fig. 23.

$$\cos\theta''_{SN} = \sin\theta_{SN} \cos\phi_{SN} \sin\theta_T \cos\phi_T + \sin\theta_{SN} \sin\phi_{SN} \sin\theta_T \sin\phi_T + \cos\theta_{SN} \cos\theta_T \quad (4.2.5)$$

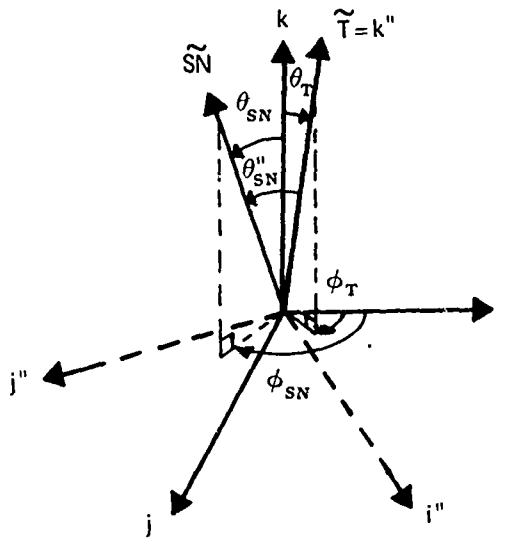


Fig. 23. Normal,  $\tilde{SN}$ , from surface reflecting sun in double prime coordinate system.

### 4.3 Sky Reflectance

The sky reflectance for the tipped wave surface is a direct extension of the equations given in Sect. 3.5 for the untipped ergodic cap sky reflectance. Eq. 3.5.1 becomes

$$\bar{N}_{sky}(\theta_p, \phi_p) = \frac{1}{A_p} \left\{ \sum_{i=1}^n \left[ \sum_{j=1}^m N(\theta_B, \phi_B)_{ij} Q^0(\theta_{Bij}) r(\theta_{BRij}) \cos\theta_{BRij} \right] \frac{A_H(\theta''_{Ni})}{\cos\theta''_{Ni}} \right\} \quad (4.3.1)$$

The expression for the horizontal area of the surface at  $\theta_N'' = 0$  is Eq. 3.5.2. The general expression for the horizontal area of each element merely substitutes  $\theta_N''$  for  $\theta_N$  in Eq. 3.5.3. Similarly the total projected area of the cap changes from Eq. 3.5.5 to

$$A_p = \sum_{i=1}^n \left[ \sum_{j=1}^m \cos \theta_{BR,j} \right] \frac{A_H(\theta_{N,i}'')}{\cos \theta_{N,i}''} \quad (4.3.2)$$

The Fresnel reflectance angle,  $\theta_{BR}$ , and the sky radiance angles,  $\theta_B, \phi_B$ , are found by first rotating to the double prime system defined by the tilt position  $\theta_T, \phi_T$ . The observers position,  $\theta_o, \phi_o$ , is found in the rotated system by substituting into Eq. 3.2.8 through 3.2.10 as follows,

$$\cos \theta_o'' = \sin \theta_o \cos \phi_o \sin \theta_T \cos \phi_T + \sin \theta_o \sin \phi_o \sin \theta_T \sin \phi_T + \cos \theta_o \cos \theta_T \quad (4.3.3)$$

$$\cos \phi_o'' = [\sin \theta_o \cos \phi_o \cos \theta_T \cos \phi_T + \sin \theta_o \sin \phi_o \cos \theta_T \sin \phi_T - \cos \theta_o \sin \theta_T] \div \sin \theta_o'' \quad (4.3.4)$$

$$\sin \phi_o'' = [-\sin \theta_o \cos \phi_o \sin \phi_T + \sin \theta_o \sin \phi_o \cos \phi_T] \div \sin \theta_o'' \quad (4.3.5)$$

See Fig. 24 for the relationships between the vector  $\tilde{O}$  and the unrotated and rotated axes.

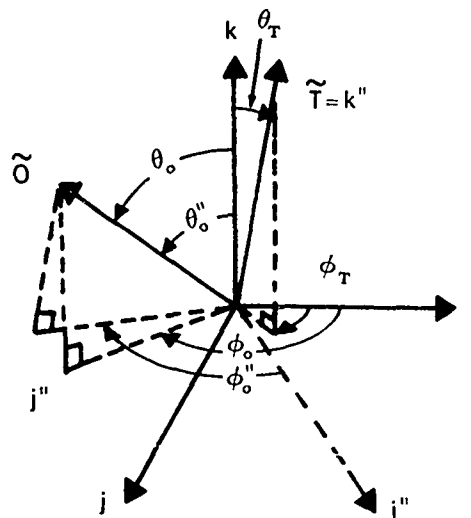


Fig. 24. Observer  $\tilde{O}$  vector, in principal and double prime system.

Now both the vector  $\tilde{O}$ , and the vectors,  $\tilde{N}$ , of the elements of the ergodic cap are in the double prime system.

The second step is to let the vector  $\tilde{O}$  (at  $\theta_o, \phi_o$  or  $\theta_o'', \phi_o''$ ) define the single prime system, and to find the vector  $\tilde{N}$  position in the single prime system through substituting into Eqs. 3.2.8 through 3.2.10. See Fig. 25.

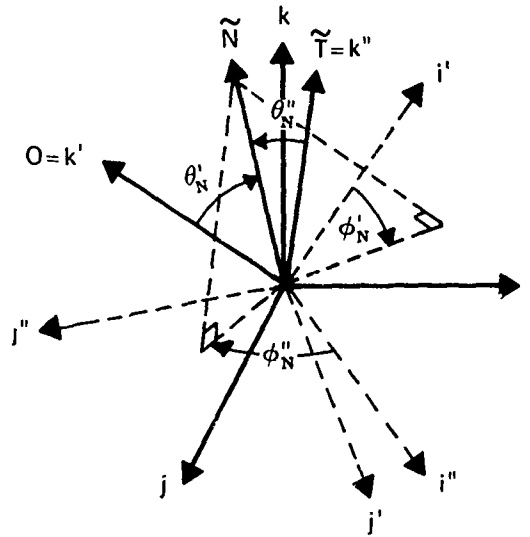


Fig. 25. Normal  $\tilde{N}$  from element of ergodic cap in double prime and prime coordinate systems.

$$\cos\theta_N' = \sin\theta_N'' \cos\phi_N'' \sin\theta_o'' \cos\phi_o'' + \sin\theta_N'' \sin\phi_N'' \sin\theta_o'' \sin\phi_o'' + \cos\theta_N'' \cos\theta_o'' \quad (4.3.6)$$

$$\cos\phi_N' = [\sin\theta_N'' \cos\phi_N'' \cos\theta_o'' \cos\phi_o'' + \sin\theta_N'' \sin\phi_N'' \cos\theta_o'' \sin\phi_o'' - \cos\theta_N'' \sin\theta_o''] \div \sin\theta_N' \quad (4.3.7)$$

$$\sin\phi_N' = [-\sin\theta_N'' \cos\phi_N'' \sin\phi_o'' + \sin\theta_N'' \sin\phi_N'' \cos\phi_o''] \div \sin\theta_N' \quad (4.3.8)$$

As before,  $\theta_N'$  is the Fresnel reflectance angle,  $\theta_{BR}$ . When  $\theta_N' \geq 90^\circ$ , the reflectance and projected area are zero and there is no contribution to the sum from that element of the ergodic cap. The radiance direction angles in the prime system are again  $\theta_B' = 2\theta_N'$  and  $\phi_B' = \phi_N'$ .

The third step is to go from the single prime system to the unrotated system through the use of Eqs. 3.5.11 through 3.5.13 as was shown in Fig. 17, section 3.5. Again when  $\theta_B > 90^\circ$ , the radiance contribution is considered negligible.

#### 4.4 Upwelling Radiance

It will be assumed that since the untilted ergodic cap represents the time- or space-averaged case, that it is also appropriate for all parts of the upwelling equation relating to the light penetrating the sea surface from above, and reflecting and interreflecting beneath the surface. The only term in which the cap is assumed tipped is the time-averaged transmittance of the radiance through the water-air surface toward the observer. Thus Eq. 3.6.1 becomes

$$\begin{aligned} \bar{N}_u(\theta_p, \phi_p) = & \left[ \int_{2\pi} N(\theta_B, \phi_B) Q^0(\theta_B) \int t(\theta_B) \cos \theta_B d\hat{t} d\Omega_B \right. \\ & \left. + \bar{N}_s(\theta_s, 0) Q^0(\theta_s) \int t(\theta_s) \cos \theta_s d\hat{t} d\Omega_s \right] \times \\ & \left[ \frac{R_\infty \int t(\theta_0'') d\hat{t}}{\pi(1-R_\infty \int r_s d\hat{t})} \left( \frac{n}{n'} \right)^2 \right] \end{aligned} \quad (4.4.1)$$

The angle toward the observer in the double prime system  $\theta_0''$ , was found in Eq. (4.3.4) in the preceding section.

#### 4.5 Directional Radiance of Tilted Sea Surface

The directional radiance of the sea surface at resolutions which do not average over large areas (or are not long time exposures), can be approximated by computing the radiance of a tipped ergodic cap. Eq. 3.7.1 is directly applicable for summing the components of the radiance. The radiances of the parts of the wave pattern would emerge from computations for ergodic caps tipped at the appropriate angles.

#### 5. REFERENCES

1. S. Q. Duntley, *Visibility of Submerged Objects*, Visibility Laboratory, Contract N5ori 07864, MIT (1952), Chap. I.
2. R. W. Preisendorfer, *Principles of Radiative Transfer in the Sea*, ms. to be published.
3. J. I. Gordon, *Determination by Computer of the Radiance (Red Light) of Waves Due to a Submerged Body* (U.) CONFIDENTIAL report. SIO Ref. 66-9 (1966).
4. H. V. Sverdrup, M. W. Johnson, and R. H. Fleming, *The Oceans*, Prentice-Hall, Inc., New York (1942) p. 55.
5. American Institute of Physics Handbook, Section 6-18, McGraw-Hill Book Company, Inc., New York (1957).

6. J. P. Riley and G. Skirrow, **Chemical Oceanography**, Vol. I., Academic Press, London and New York (1965), p. 108.
7. R. W. Austin and J. M. Hood, Jr., *Optical Measurement of WESTPAC Coastal Waters*, (U.) CONFIDENTIAL report. Proceedings, Third U. S. Navy Symposium on Military Oceanography, Vol. I (1966).
8. S. Q. Duntley, **Visibility Studies and Some Applications in the Field of Camouflage**, Summary Tech. Rept. of Division 16, NDRC (Columbia Univ. Press, New York, 1946), Vol. 2, p. 212.
9. S. Q. Duntley, **Reflectance of Natural Terrains**, Louis Comfort Tiffany Found., Oyster Bay, L.I., New York (14 Sept. 1945), p. 62.
10. S. Q. Duntley, *Light in the Sea*, J. Opt. Soc. Am. **53**, 214 (1963).
11. F. S. Johnson, *The Solar Constant*, J. Meteor., **11**, No. 6, 431 (1954).
12. D. B. Judd, *Fresnel Reflection of Diffusely Incident Light*, NBS Research Paper RP-1504, J. Res. Nat'l. Bur. Std., **29**, (1942), p. 330.
13. A. Gershun, *The Light Field*, J. Math. and Phys., **18**, 51, (1939).
14. Ref. 1 and S. Q. Duntley, *Measurements of the Distribution of Water Wave Slopes*, J. Opt. Soc. Am., **44**, 574 (1954).
15. C. Cox and W. Munk, *Measurement of the Roughness of the Sea Surface from Photographs of the Sun's Glitter*, J. Opt. Soc. Am., **44**, 838 (1954).
16. W. J. Pierson, **Models of Random Seas Based on Lagrangian Equations of Motion**, N.Y.U. College of Eng. Res. Div. April (1961).

## APPENDIX A

### DERIVATION OF EQUATIONS FOR THE TRANSFORMATION OF ROTATION OF AXES EXPRESSED IN SPHERICAL COORDINATES

By J. W. Wasserboehr and J. I. Gordon

The basic equations used for the development of the angular relationships were those for the transformation of rotation\* of axis in a three dimensional rectangular coordinate vector system.

The equations are:

$$\begin{aligned}x &= x'(i \cdot i') + y'(i \cdot j') + z'(i \cdot k') \\y &= x'(j \cdot i') + y'(j \cdot j') + z'(j \cdot k') \\z &= x'(k \cdot i') + y'(k \cdot j') + z'(k \cdot k')\end{aligned}\quad \text{Group (A.1)}$$

and,

$$\begin{aligned}x' &= x(i \cdot i') + y(j \cdot i') + z(k \cdot i') \\y' &= x(i \cdot j') + y(j \cdot j') + z(k \cdot j') \\z' &= x(i \cdot k') + y(j \cdot k') + z(k \cdot k')\end{aligned}\quad \text{Group (A.2)}$$

If the rectangular coordinate system is changed to the spherical coordinate system of Figure A.1 it can be seen that,

$$\begin{aligned}x &= \rho \sin\theta \cos\phi & x' &= \rho \sin\theta' \cos\phi' \\y &= \rho \sin\theta \sin\phi & y' &= \rho \sin\theta' \sin\phi' \\z &= \rho \cos\theta & z' &= \rho \cos\theta'\end{aligned}\quad \text{Group (A.3)}$$

and if these are substituted into groups (A.1) and (A.2), and the common factor  $\rho$  is divided out, the equations of transformation of rotation become,

$$\begin{aligned}\sin\theta \cos\phi &= \sin\theta' \cos\phi' (i \cdot i') + \sin\theta' \sin\phi' (i \cdot j') + \cos\theta' (i \cdot k') \\ \sin\theta \sin\phi &= \sin\theta' \cos\phi' (j \cdot i') + \sin\theta' \sin\phi' (j \cdot j') + \cos\theta' (j \cdot k') \\ \cos\theta &= \sin\theta' \cos\phi' (k \cdot i') + \sin\theta' \sin\phi' (k \cdot j') + \cos\theta' (k \cdot k')\end{aligned}\quad \text{Group (A.4)}$$

\* I. S. Sokolnikoff, and E. S. Sokolnikoff, *Higher Mathematics for Engineers and Physicists*, McGraw-Hill, N. Y., 2nd Ed., 1941, p. 403.

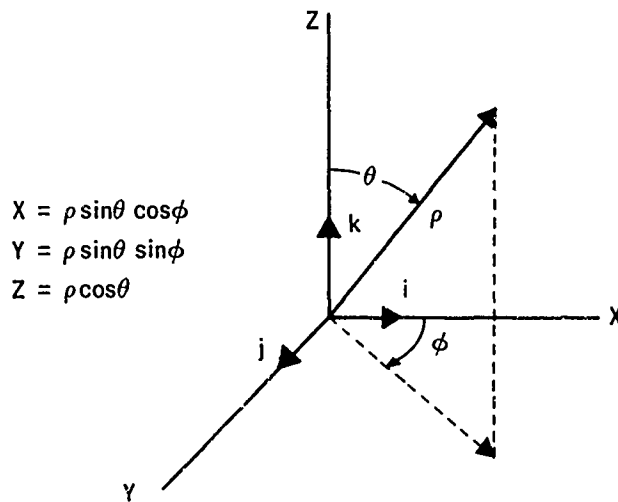


Fig. A.1. Rectangular Coordinate System to Spherical Coordinate System.

and,

$$\begin{aligned}
 \sin \theta' \cos \phi' &= \sin \theta \cos \phi (i \cdot i') + \sin \theta \sin \phi (j \cdot i') + \cos \theta (k \cdot i') \\
 \sin \theta' \sin \phi' &= \sin \theta \cos \phi (i \cdot j') + \sin \theta \sin \phi (j \cdot j') + \cos \theta (k \cdot j') \\
 \cos \theta' &= \sin \theta \cos \phi (i \cdot k') + \sin \theta \sin \phi (j \cdot k') + \cos \theta (k \cdot k')
 \end{aligned}$$

Group (A.5)

In spherical coordinates the  $i$ ,  $j$ , and  $k$  unit vectors are:

$$\begin{aligned}
 i; \rho &= 1, \theta = 90^\circ, \phi = 0^\circ \\
 j; \rho &= 1, \theta = 90^\circ, \phi = 90^\circ \\
 k; \rho &= 1, \theta = 0^\circ, \phi = 0^\circ
 \end{aligned}$$

From these it is obvious that,

$$\begin{aligned}
 i &= (1)i + (0)j + (0)k = i \\
 j &= (0)i + (1)j + (0)k = j \\
 k &= (0)i + (0)j + (1)k = k
 \end{aligned}$$

Group (A.6)

If  $\theta_1$  and  $\phi_1$  are the angles for the transformation of rotation to the new axes  $x'$ ,  $y'$  and  $z'$  (Figure A.2) then the spherical coordinates of  $i'$ ,  $j'$ , and  $k'$ , with respect to the original  $x$ ,  $y$ , and  $z$  systems are:

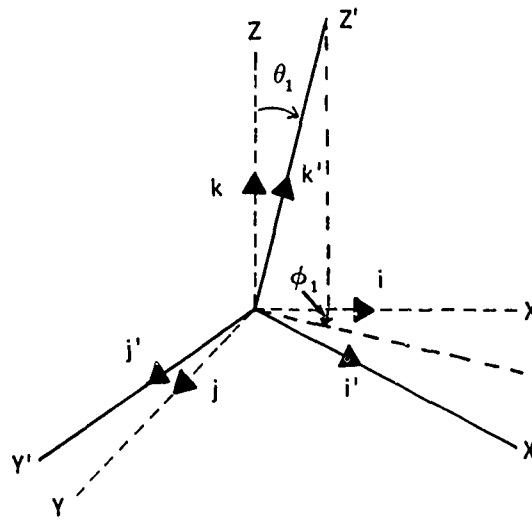
$$\begin{aligned} i' &; \rho = 1, \theta = \theta_1 + 90^\circ, \phi = \phi_1 \\ j' &; \rho = 1, \theta = 90^\circ, \phi = \phi_1 + 90^\circ \\ k' &; \rho = 1, \theta = \theta_1, \phi = \phi_1 \end{aligned}$$

If these latter values are substituted into the general equation of a vector,

$$\tilde{A} = xi + yj + zk = (\rho \sin \theta \cos \phi)i + (\rho \sin \theta \sin \phi)j + (\rho \cos \theta)k \quad \text{Group (A.7)}$$

then equations for the vectors  $i'$ ,  $j'$ , and  $k'$  in relation to the original

Fig. A.2. Rotation of Axes.



system are obtained as follows:

$$\begin{aligned} i' &= [\sin(\theta_1 + 90)\cos\phi_1]i + [\sin(\theta_1 + 90)\sin\phi_1]j + [\cos(\theta_1 + 90)]k \\ j' &= [\sin 90 + \cos(\phi_1 + 90)]i + [\sin 90 \sin(\phi_1 + 90)]j + [\cos 90]k \\ k' &= [\sin\theta_1, \cos\phi_1]i + [\sin\theta_1 \sin\phi_1]j + [\cos\theta_1]k \end{aligned} \quad \text{Group (A.8)}$$

and  $\sin 90^\circ = 1$ ,  $\cos 90^\circ = 0$ ,  $\sin(\theta_1 + 90) = \cos\theta_1$ ; and  $\cos(\theta_1 + 90) = -\sin\theta_1$

$$\begin{aligned} i' &= (\cos\theta_1 \cos\phi_1)i + (\cos\theta_1 \sin\phi_1)j - (\sin\theta_1)k \\ j' &= -(\sin\phi_1)i + (\cos\phi_1)j + (0)k \\ k' &= (\sin\theta_1 \cos\phi_1)i + (\sin\theta_1 \sin\phi_1)j + (\cos\theta_1)k \end{aligned} \quad \text{Group (A.9)}$$



From vector analysis the dot product of any two vectors is  $\tilde{A} \cdot \tilde{B} = x_a x_b + y_a y_b + z_a z_b$ , therefore,

$$i \cdot i' = (1) (\cos\theta_1 \cos\phi_1) + 0 + 0 = \cos\theta_1 \cos\phi_1$$

$$i \cdot j' = (1) (-\sin\phi_1) + 0 + 0 = -\sin\phi_1$$

$$i \cdot k' = (1) (\sin\theta_1 \cos\phi_1) + 0 + 0 = \sin\theta_1 \cos\phi_1$$

$$j \cdot i' = 0 + (1) (\cos\theta_1 \sin\phi_1) + 0 = \cos\theta_1 \sin\phi_1$$

$$j \cdot j' = 0 + (1) (\cos\phi_1) + 0 = \cos\phi_1$$

Group (A.10)

$$j \cdot k' = 0 + (1) (\sin\theta_1 + \sin\phi_1) + 0 = \sin\theta_1 \sin\phi_1$$

$$k \cdot i' = 0 + 0 + (1) (-\sin\theta_1) = -\sin\theta_1$$

$$k \cdot j' = 0 + 0 + (1) (0) = 0$$

$$k \cdot k' = 0 + 0 + (1) (\cos\theta_1) = \cos\theta_1$$

Substituting these dot product values into the group equations (A.4) and (A.5), the following are obtained.

$$\sin\theta \cos\phi = \sin\theta' \cos\phi' \cos\theta_1 \cos\phi_1 - \sin\theta' \sin\phi' \sin\phi_1 + \cos\theta' \sin\theta_1 \cos\phi_1$$

$$\sin\theta \sin\phi = \sin\theta' \cos\phi' \cos\theta_1 \sin\phi_1 + \sin\theta' \sin\phi' \cos\phi_1 + \cos\theta' \sin\theta_1 \sin\phi_1$$

Group (A.11)

$$\cos\theta = -\sin\theta' \cos\phi' \sin\theta_1 + \cos\theta' \cos\theta_1$$

and,

$$\sin\theta' \cos\phi' = \sin\theta \cos\phi \cos\theta_1 \cos\phi_1 + \sin\theta \sin\phi \cos\theta_1 \sin\phi_1 - \cos\theta \sin\theta_1$$

$$\sin\theta' \sin\phi' = -\sin\theta \cos\phi \sin\phi_1 + \sin\theta \sin\phi \cos\phi_1$$

Group (A.12)

$$\cos\theta' = \sin\theta \cos\phi \sin\theta_1 \cos\phi_1 + \sin\theta \sin\phi \sin\theta_1 \sin\phi_1 + \cos\theta \cos\theta_1$$

## OCCLUSION

by Keith B. MacAdam

The theory of occlusion is given in Reference 2, Chapter 12. The problem will be stated, definitions and terminology given, and some results derived.

## Definition

$Q^\circ(\hat{x}, \xi)$  is the average fractional time that an incident path  $\xi$  corresponds to direct light from the sky or sun at point  $\hat{x}$  on the mean sea surface  $\hat{S}$ . As the waves undulate, the intersection  $x$  of the path of sight  $\xi$  with  $S$  changes its horizontal position; Fig. B.1.

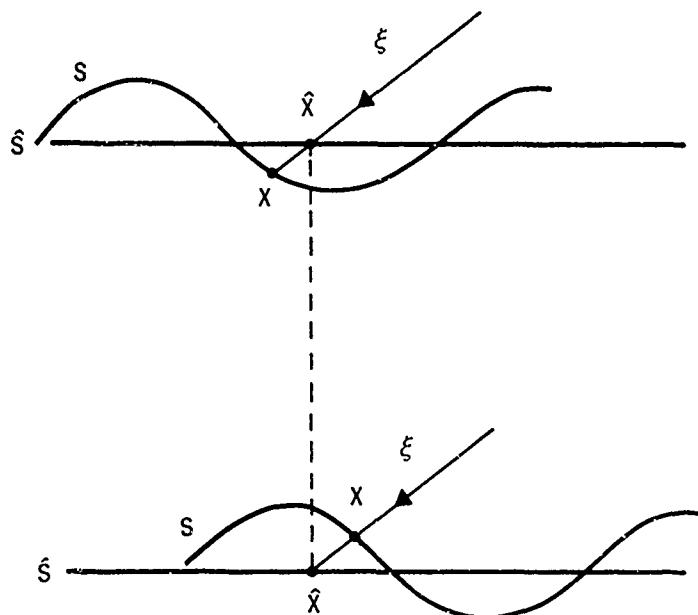


Fig. B.1

On the assumption that the sea surface elevations  $\zeta$  at neighboring points  $\hat{x}$  are uncorrelated, it can be imagined that what is seen from  $\xi$  is the air-water interface point directly above or below  $\hat{x}$ , with no change in results, Fig. B.2.

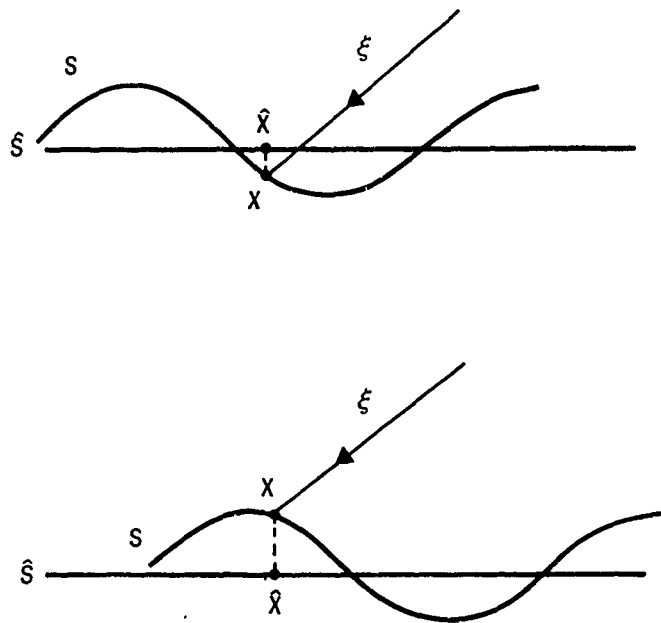


Fig. B.2

The problem can be visualized as follows: How often could one see a floating bob at horizontal point  $\hat{x}$ ? (Indeed, this point of view yields an immediate technique for empirical verification of the theory).

There is a certain probability  $p_1(\zeta)\Delta\zeta$  that  $x$  will fall into the vertical interval  $(\zeta, \zeta + \Delta\zeta)$ . Whenever it falls, there is a certain probability that  $\xi$  has no additional intersections with  $S$  between  $x$  and the sky.

If  $p_2(\zeta, \Delta\zeta)$  is the probability that in an increment  $\Delta\zeta$  of vertical ascent along  $\xi$  there is no intersection, then

$$\prod p_2(\zeta, \Delta\zeta)$$

is the probability that  $\xi$  is completely free of intersections. Then the final answer is

$$Q^0 = \sum p_1(\zeta) \Delta\zeta \left[ \prod p_2(\zeta, \Delta\zeta) \right] \quad (B.1)$$

In the following, it is assumed that the Neumann spectrum, developed in Ref. 2 satisfactorily represents the ocean surface, although it is essential only that the mathematical form of the Neumann spectrum agree with experiment.

From the Neumann spectrum,

$$p_1(\zeta) \Delta \zeta = \frac{1}{\sqrt{2\pi m_{00}}} \exp\left(-\frac{\zeta^2}{2m_{00}}\right) \Delta \zeta \quad (\text{B.2})$$

where  $m_{00}$  is the mean square wave height.

From the Neumann spectrum it is also possible to obtain the average number of times per unit length that a horizontal path at height  $\zeta$  from the mean sea surface crosses the air-water interface. That is,

$$n(\zeta) = \frac{1}{\pi} \left[ \frac{m_{20}}{m_{00}} \right]^{1/2} \exp - \frac{\zeta^2}{2m_{00}} \quad (\text{B.3})$$

where  $m_{20} = \sigma^2$ , the mean square wave slope. Assuming that ideas from the Poisson distribution describing random events may be used, the probability that a horizontal path of length  $\Delta x$  is free of intersections is  $\exp(-n(\zeta) \Delta x)$ .

Then if the slanted path  $\xi$  is approximated by a series of short horizontal paths at increasing height, the result is the approximation

$$\prod p_2(\zeta, \Delta \zeta) = \prod_{j=0}^{\infty} \exp \left[ -n(\zeta_j) \Delta \zeta / \tan \psi \right] \quad (\text{B.4})$$

since  $\Delta \zeta = \Delta x \tan \psi$ .  $\psi$  is the elevation angle. This is a procedure similar to that used in Ref. 2. Then

$$\prod p_2(\zeta, \Delta \zeta) = \prod_{j=0}^{\infty} \exp \left[ -n(\zeta_0 + j \Delta x \tan \psi) \Delta \zeta / \tan \psi \right] \quad (\text{B.5})$$

$$= \exp \left\{ \sum_{j=0}^{\infty} -n(\zeta_0 + j \Delta x \tan \psi) \Delta \zeta / \tan \psi \right\} \quad (\text{B.6})$$

Now setting  $\zeta = \zeta_0 + j \Delta x \tan \psi$ , and letting  $\Delta x \rightarrow 0$

$$\prod = \exp \left\{ \frac{-1}{\tan \psi} \int_{\zeta_0}^{\infty} n(\zeta) d\zeta \right\}. \quad (\text{B.7})$$

Upon evaluation

$$\Pi = \exp \left\{ - \frac{\sqrt{m_{20}}}{\sqrt{2\pi} \tan \psi} \left[ 1 - E(\zeta_0 / \sqrt{m_{00}}) \right] \right\} \quad (\text{B.8})$$

where

$$E(t) = \int_{-t}^t \frac{1}{\sqrt{2\pi}} \exp \left( -\alpha^2/2 \right) d\alpha \quad (\text{B.9})$$

Also,

$$Q^\circ = \sum p_1(\zeta) \Delta \zeta \Pi \quad (\text{B.10})$$

becomes the integral

$$\int_{-\infty}^{\infty} p_1(\zeta) \Pi d\zeta \quad (\text{B.11})$$

and

$$Q^\circ = \int_{-\infty}^{\infty} \frac{1}{\sqrt{2\pi m_{00}}} \exp \left( -\zeta_0^2 / 2m_{00} \right) \exp \left[ - \frac{\sqrt{m_{20}}}{\tan \psi \sqrt{2\pi}} \left\{ 1 - E(\zeta_0 / \sqrt{m_{00}}) \right\} \right] d\zeta_0 \quad (\text{B.12})$$

The result is independent of  $m_{00}$  and can be written

$$Q^\circ = \int_{-\infty}^{\infty} \frac{1}{\sqrt{2\pi}} \exp \left( -\eta^2/2 \right) \exp \left[ - \frac{\sigma}{\tan \psi \sqrt{2\pi}} (1 - E(\eta)) \right] d\eta. \quad (\text{B.13})$$

$Q^\circ$  is the value of a modified error integral, parametrized by  $\sigma$  and  $\psi$ . Some simplifications of this difficult integral are possible.

$$Q^\circ = \frac{\exp \left( - \frac{\sigma}{\tan \psi \sqrt{2\pi}} \right)}{2\pi} \int_{-\infty}^{\infty} \exp \left[ \frac{\sigma E(\eta)}{\tan \psi \sqrt{2\pi}} - \frac{\eta^2}{2} \right] d\eta \quad (\text{B.14})$$

Now notice that  $E(\eta) = -E(-\eta)$ . Then

$$\int_{-\infty}^{\infty} = \int_0^{\infty} + \int_{-\infty}^0 = \int_0^{\infty} \left[ \exp \frac{\sigma E(\eta)}{\tan \psi \sqrt{2\pi}} + \exp \frac{-\sigma E(\eta)}{\tan \psi \sqrt{2\pi}} \right] \exp \left( -\frac{\eta^2}{2} \right) d\eta \quad (\text{B.15})$$

$$= 2 \int_0^{\infty} \cosh \left[ \frac{\sigma E(\eta)}{\tan \psi \sqrt{2\pi}} \right] \exp \left( -\frac{\eta^2}{2} \right) d\eta \quad (B.16)$$

Then

$$Q^0 = \exp \left( \frac{-\sigma}{\tan \psi \sqrt{2\pi}} \right) \int_0^{\infty} \frac{2}{\sqrt{2\pi}} \cosh \left[ \frac{\sigma E(\eta)}{\tan \psi \sqrt{2\pi}} \right] \exp \left( -\frac{\eta^2}{2} \right) d\eta \quad (B.17)$$

Except for the hyperbolic cosine factor, the integral is the error integral with value 1. How large is the effect of the extra factor? For suns higher than  $\psi = 10^\circ$ , in the worst case,  $v = 38$  knots, the actual integral is less than 12% greater than 1, and probably better than this; for  $v = 26$  the actual integral is less than 1.08. For suns higher than  $\psi = 20^\circ$  the integral is less than 1.03 for all wind-speeds less than or equal to 38.

Then for  $10^\circ \leq \psi \leq 90^\circ$  and  $0 \leq v \leq 38$  the formula below may be used

$$Q^0 = \exp \left[ -\sigma / (\sqrt{2\pi} \tan \psi) \right] \quad (B.18)$$

It will be good to within 12%. In all cases the actual value of  $Q^0$  will be greater than that given above, within the specified limit.

It is interesting to note that if the probability is computed that a single path  $\xi$  leaving  $\hat{S}$  has no intersection with  $S$ , i.e., if  $\xi$  is tied to the mean surface rather than the actual surface B.18 is obtained exactly.

UNCLASSIFIED  
Security Classification

DOCUMENT CONTROL DATA - R&D		
<i>(Security classification of title, body of abstract and summary, classification must be entered when the overall report is classified)</i>		
1. ORIGINATING ACTIVITY (Corporate author) Visibility Laboratory University of California San Diego, California 92152		2a. REPORT SECURITY CLASSIFICATION UNCLASSIFIED
		2b. GROUP
3. REPORT TITLE  DIRECTIONAL RADIANCE (LUMINANCE) OF THE SEA SURFACE		
4. DESCRIPTIVE NOTES (Type of report and inclusive dates)		
5. AUTHOR(S) (Last name, first name, initial)  Gordon, Jacqueline I.		
6. REPORT DATE October 1969	7a. TOTAL NO. OF PAGES 50	7b. NO. OF REFS 16
8a. CONTRACT OR GRANT NO. N00024-68-C-1100	9a. ORIGINATOR'S REPORT NUMBER(S)  SIC Ref. 63 20	
b. Task I		
c.		
d.	9b. OTHER REPORT NO(S) (Any other numbers that may be assigned this report)	
10. AVAILABILITY LIMITATION NOTICES  Distributio this document is unlimited.		
11. SUPPLEMENTARY NOTES		12. SPONSORING MILITARY ACTIVITY Naval Ship Systems Command Department of the Navy Washington, D. C. 20360
13. ABSTRACT  The development of the equations for the computation of directional sea radiance and/or luminance are presented. Three types of conditions for which calculations may be made are each treated separately: first, the radiance or luminance of the calm sea; second, the radiance or luminance of the time- or space-averaged wind-ruffled sea; and third, the radiance or luminance of the sea surface in which large wave pattern is resolved but small capillary waves are unresolved. ( )  ↑		

DD FORM 1473  
1 JAN 64

UNCLASSIFIED  
Security Classification

14	KEY WORDS	LINK A		LINK B		LINK C	
		ROLE	WT	ROLL		WT	WT
	Directional Radiance Directional Luminance Sea Surface Radiance						